Pyrite-lined shells as indicators of limited oxygen exposure time and inefficient bioirrigation in the Holocene-Anthropocene stratigraphic record

Adam Tomašových[1], Michaela Berensmeier[2], Ivo Gallmetzer[2], Alexandra Haselmair[2], Martin Zuschin[2]

[1]Earth Science Institute, Slovak Academy of Sciences, Bratislava, 84005, Slovakia
[2]University of Vienna, Department of Palaeontology, Althanstrasse 14, 1090 Vienna, Austria

Correspondence to: Adam Tomašových (geoltoma@savba.sk)

Abstract. Although the depth of bioturbation can be estimated on the basis of ichnofabric, the time scale of sediment mixing and irrigation by burrowers that affects carbonate preservation and biogeochemical cycles is difficult to estimate in the stratigraphic record. However, pyrite linings on interior of shells can be a signature of slow mixing and irrigation rate because they indicate that shells of molluscs initially inhabiting oxic sediment zones were immediately and permanently sequestered in reduced microenvironments where molluscan biomass and associated microbial coatings stimulated sulfate reduction and pyrite precipitation. A high abundance of pyrite-lined shells in the stratigraphic record can thus be diagnostic of limited net exposure of labile tissues to O_2 even when the seafloor is inhabited by abundant burrowing infauna as in the present-day northern Adriatic Sea. Here, we reconstruct this sequestration pathway (1) by assessing preservation and postmortem ages of pyrite-lined shells of the hypoxia-tolerant bivalve *Varicorbula gibba* in sediment cores and (2) by evaluating whether an independently-documented decline in bioturbation, driven by eutrophication and seasonal hypoxia during the 20th century, affected the frequency of pyrite-lined shells in the stratigraphic record of the northern Adriatic Sea. First, at prodelta sites with high sedimentation rate, linings of pyrite framboids form rapidly in near-surface sediment zones as they appear already in interiors of shells and in intra-shell conchiolin layers younger than 10 years and occur preferentially in well-preserved and articulated shells with periostracum and relatively high concentrations of amino acids. Second, increments deposited in the early 20th century contain <20% of shells with pyrite at the Po prodelta and 30-40% at the Isonzo prodelta, whereas the late 20th century increments possess 50-80% of shells with pyrite at both locations. At sites with slow sedimentation rate, the frequency of pyrite linings is low (<10-20%). Third, the upcore increase in the frequency of pyrite-lined shells positively correlates with an abrupt increase in maximum shell size and biomass of *V. gibba*. Therefore, the upcore increase in the frequency of pyrite-lined shells indicates that sediment mixing and bioirrigation rates declined during the 20th century, leading to higher sequestration of pyrite-lined shells during the late 20th century. We hypothesize that the permanent preservation of pyrite linings within the shells of *V. gibba* in the subsurface stratigraphic record was allowed by slow recovery of infaunal communities frequently interrupted by seasonal hypoxic events, leading to the dominance of surficial sediment modifiers with low irrigation potential. Abundance of well-preserved shells lined by pyrite exceeding ~10% per assemblage in apparently well-mixed sediments in the deep-time stratigraphic record can be an indicator of short net exposure of shells to O_2 and inefficient bioirrigation. Fine-grained prodelta sediments in the northern Adriatic Sea deposited since the mid-20th century, with high preservation potential of reduced microniches, can represent taphonomic and early-diagenetic analogues of deep-time skeletal assemblages with pyrite linings.

1. Introduction

Slow and shallow bioturbation (including biomixing and bioirrigation, Kristensen et al., 2012) can reflect oxygen depletion, toxicity or other environmental stresses that limit ecosystem functioning and nutrient recycling (Rhoads and Germano, 1986; Nilsson and Rosenberg, 2000; Rosenberg et al., 2001; Solan and Kennedy, 2002). It can be also conditioned by evolutionary

factors such as the lack of innovations for deep burrowing (Thayer, 1983) or by extinction of burrowers after mass

40   extinctions (Pruss et al., 2004; Buatois and Mangano, 2011). Estimating the mixing rate and depth on the basis of the stratigraphic record thus can be used to assess the response and recovery of benthic ecosystems to stress and disturbances and to evaluate long-term trends in ecosystem functioning and biogeochemical cycling (Droser et al., 2002; Canfield and Farquhar, 2009; Tarhan et al., 2015; Gougeon et al., 2018; Buatois et al., 2020). The mixing rate, the mixing depth, and the sediment accumulation rate represent three parameters that determine the residence time of sedimentary and organic particles

45   in the mixed layer (Meysman et al., 2003). The residence time determines preservation, recycling and burial efficiency of organic matter, carbonates and redox-sensitive minerals because it controls their exposure time to O_2 in near-surface sediment zones (Aller, 1994; Hartnett et al., 1998; Meile and van Cappellen, 2005; Boyle et al., 2014; Aller and Cochran, 2019) and to borers, microbes and undersaturated pore waters in the so-called taphonomic active zone (TAZ; Davies et al., 1989; Walker and Goldstein, 1999). If sedimentation rate does not change over a given duration of deposition, dividing the

50   depth of the mixed layer by sediment accumulation rate can be used to estimate the residence time of particles in the mixed layer (Wheatcroft, 1990; Tomašových et al., 2019a). However, first, exposure time to bioirrigation is not a simple function of residence time of sedimentary particles in the mixed layer and also depends on the size, life habits and mobility of burrowers (Sandnes et al., 2000; Lohrer et al., 2004; Gingras et al., 2008; Renz et al., 2018), with deposit feeders mainly promoting mixing and suspension-feeders and chemosymbionts mainly inducing irrigation (Christensen et al., 2000). Second, long-term

55   estimates of net sediment accumulation rate cannot be interpolated to shorter time scales (Jerolmack and Sadler, 2007) and the time scale of mixed-layer formation is similarly confounded by internal temporal variability in bioturbation over shorter time scales (Teal et al., 2008). For example, a 20-cm thick layer deposited under 1 cm/y may be mixed (or irrigated) instantaneously just in a single year or permanently over 20 years. Both the instantaneous mixing and the slower mixing will generate age-homogeneous distribution of sedimentary particles but will differ in recycling and burial efficiency of redox-

60   sensitive sedimentary particles. Therefore, although the depth of mixing in the stratigraphic record can be estimated on the basis of ichnofabric and trace fossils (Droser and Bottjer, 1988; Savrda and Ozalas, 1993), it is unclear whether intense mixing, leading to age homogenization, was also associated with efficient irrigation and whether a mixed layer observed in the stratigraphic record was mixed instantaneously or whether the ichnofabric developed over yearly, decadal or longer time scales. This uncertainty differs from temporally-explicit estimates of O_2 penetration, from estimates of apparent redox

65   potential discontinuity, or from the estimates of the mixed layer thickness based on [234]Th that can be measured in present-day environments (Maire et al., 2008; Germano et al., 2011; Gerwing et al., 2018; Solan et al., 2019).

One criterion that can be used to constrain the residence time of particles and their exposure to O_2 in the mixed layer in the *ancient* stratigraphic record includes the detection of rapid authigenic mineralization associated with the decay of labile organic tissues in the absence of O_2 (Allison, 1988; Briggs et al., 1991, 1996). The lack of bioturbation that limit O_2

70   exposure and allow preservation of intact, articulated, multi-element skeletal remains under anaerobic degradation of organic matter can induce early pyritization, phosphatization or silicification of organic tissues (Gabbott et al., 2004; Zhu et al., 2005; Cai et al., 2012; Saleh et al., 2019; 2020; Schiffbauer et al., 2014; Novek et al., 2016). Early pyritization or silicification induced by reactive organics may also generate death masks that stabilize and cement sediment and blanket benthic organisms (Gehling, 1999; Strang et al., 2016; Tarhan et al., 2016; Gibson et al., 2018; Liu et al., 2019; Slagter et al.,

75   2020). Similar pathways stimulated by the decay of labile organics or further sustained by microbial and mucus-forming processes in anaerobic microniches (Emery and Rittenberg, 1952; Jorgensen, 1977; Borkow and Babcock, 2003; Stockdale et al., 2010; Anderson et al., 2011; Virtasalo et al., 2010, 2013; Lehto et al., 2014) do not directly replace organic tissues but can lead to distinctive clusters of authigenic minerals concentrated in intra-skeletal voids initially filled with organic tissues in otherwise well-preserved skeletal remains (Brett et al., 2012a, b). For example, intraskeletal pores (initially containing

80   labile organic tissues and microbes associated with their decay) lined by framboids or larger pyrite crystals preserved in the

stratigraphic record, as observed in interiors of foraminifers, cephalopods, articulated brachiopods or bivalves, demonstrate that reduced microniches were not re-exposed to O_2 by irrigation or exhumed to sediment-water interface (Hudson, 1982; Schieber and Baird, 2001; Hunda et al., 2006; Schieber, 2012; Machain-Castillo et al., 2019). Such microniches thus remained permanently sequestered after their initial formation. However, with the exception of seep environments (Powell et

85 al. 2012) or studies focusing on pyrite infills in burrows (Virtasalo et al., 2010), pyrite-lined skeletal remains are rarely documented or observed in actualistic studies assessing preservation of organisms with durable skeletal elements in Holocene or Anthropocene marine environments (Best and Kidwell, 2000). This rarity may be not surprising because the preservation of pyrite framboids nucleating at the sites of organic decay (initiated in reduced microniches) is limited in habitats affected by physical mixing or bioturbation where most of the sulfide produced by sulfate reducers in microniches is

90 later re-oxidized (Canfield et al., 1993; Wijsman et al., 2002; Canfield and Farquhar, 2009). However, taphonomic and early-diagenetic pathways that affect skeletal remains remain poorly explored in environments affected by eutrophication, stratification and oxygen depletion that can be characterized by high burial efficiency of iron (Carstensen et al., 2014; Lenstra et al., 2019).

The decline in the functioning of marine soft-bottom benthic ecosystems driven by eutrophication and

95 deoxygenation over the past centuries (Schaffner et al., 1992; Valente and Cuomo, 2005; Zillén et al., 2008) thus represents a unique opportunity (1) to assess the nature of pathways that lead to the preservation of pyrite-lined shells (especially the steps associated with the initial formation of microniches and with the subsequent lack of their re-oxidation) and thus can provide a taphonomic and early-diagenetic analogues for pyrite-lined shells in the deep-time stratigraphic record, and (2) to test whether the decline in bioturbation detected in sediment cores over the past decades influenced the frequency of pyrite-

100 lined shells in the stratigraphic record. Here, we focus on Holocene-Anthropocene sediment cores from the northern Adriatic Sea which harbors diverse types of infaunal and epifaunal benthic communities (Fedra et al., 1976; Zuschin et al., 1999; Zuschin and Stachowitsch, 2009). This sea was affected by eutrophication and by an increase in frequency of seasonal hypoxia in the 20th century (Justic, 1991; Degobbis et al., 2000), with frequent mucilage events (Cozzi et al., 2004; Giani et al., 2005; Precali et al., 2005) and several spatially-extensive seasonal anoxic events inducing mass mortality of benthic

105 fauna in the 70s-90s (Stefanon and Boldrin, 1982; Stachowitsch, 1991). Oligotrophization was detected in the northern Adriatic Sea since 1990s (Djakovac et al., 2015), although habitats close to Po prodelta were regularly affected by seasonal hypoxia during the 1977-2008 monitoring (Alvisi and Cozzi, 2016) and hypoxic events were detected in the Gulf of Trieste also in the early 21st century (Kralj et al., 2020). Paleoecological records in sediment cores collected in the Po prodelta and in the Gulf of Trieste showed that the effects of seasonal oxygen depletion (and other changes related to pollution, sediment turbidity and trawling) translated into a 20th century regime shift in the composition of soft-bottom molluscan communities

110 (at 10-30 m water depths, Tomašových et al., 2020).

Pyrite can precipitate rapidly at the location of decay of primary reactive tissues of hosts or at the location of intra-skeletal organic matrices among crystals (we call such pyrite *primary linings*, Boekschoten, 1966; Brown, 1966) but can also form at the location of decay of secondary inhabitants of shells that were exposed to redox fluctuations in the taphonomic

115 active zone for longer (coelobionts, encrusters, or borers; *secondary linings*, Kobluk and Risk, 1977) or can precipitate slowly when H_2S reacts with less reactive iron-bearing minerals (Neumann et al., 2005). However, only primary linings can represent a key evidence of limited exposure time of such shells to O_2 from irrigation prior to their burial below the mixed layer. Here, to assess whether abundant pyrite-lined shells of the hypoxia-tolerant bivalve *Varicorbula gibba* are informative about mixing and irrigation rates and to distinguish primary from secondary linings (and from other types of pyrite

120 associated with skeletal remains that forms over longer time scales), we evaluate (1) the rate of pyrite formation and the depth of its formation (in surface or subsurface sediment zones) on the basis of postmortem age- and depth-frequency

distributions of dated specimens of *V. gibba* in sediment cores, (2) whether pyrite-lined valves possess more frequently a periostracum (or internal conchiolin layer) and higher shell organic content than valves without pyrite (controlling for shell postmortem age), (3) whether the increment-level frequency of pyrite-lined valves correlates negatively with other types of

125   alteration such as disarticulation or bioerosion, (4) whether the frequencies of pyrite-lined valves change upcore within the Holocene-Anthropocene stratigraphic record, and whether they track independently-documented changes in community composition and bioturbation using abundance, shell size, and biomass of the hypoxia-tolerant bivalve *V. gibba*.

2. Setting

130   The northern Adriatic Sea is a relatively low-energy shelf environment with narrow tidal range, with counterclockwise surface circulation, mainly driven by the freshwater input of the River Po (Kemp et al., 1999; Boldrin et al., 2009; Brush et al., 2021). The cyclonic circulation normally deflects nutrient-rich water masses off the Po Delta southwards. However, this circulation slows down during the summer when a local cyclonic gyre can spread such eutrophic waters also towards the eastern Adriatic shelf normally characterized by oligotrophic surface conditions. The decline in circulation leads to the

135   development of a pycnocline, and in combination with high phytoplankton production, to the accumulation of marine snow and mucilages and to bottom-water oxygen depletion in some years across large parts of the northern Adriatic Sea (Stachowitsch, 1991; Penna et al., 1993; Precali et al., 2005). Sediments associated with silt and clay-rich sediments are relatively rich in iron in deltaic environments (3-4%, Spagnoli et al., 2014%) and less so in carbonate sediments off Istria (>1.5-3% in the Gulf of Trieste, Faganeli et al., 1991; Faganeli et al., 1994; Dolenec et al., 1998). Iron is bounded mainly by

140   iron oxides or by pyrite (as framboids or foram infillings) that forms 2-5% of the sediments in the Gulf of Trieste (Faganeli and Ogrinc, 2009), and typically less than 1% in Holocene cores on the Po Plain (Amorosi et al., 2002). Biogeochemical studies performed in the 1990s showed that organic-rich sediments at Po prodelta are dominated by anaerobic decomposition of organics (mainly sulfate reduction, Barbanti et al., 1995). In contrast, less-organic rich sites in the NW Adriatic Sea with slower sedimentation display a higher importance of aerobic respiration and iron reduction (Barbanti et al., 1995; Hammond

145   et al., 1999). This gradient in sedimentation rate leads to lower recycling of organic carbon at the Po prodelta and higher recycling at distal sites. A similar situation was also observed in the Gulf of Trieste, with higher burial efficiency of organic carbon and nitrogen at muddy sites at the Isonzo prodelta and higher recycling at sandy sites with slow sedimentation in the southern parts of the Gulf of Trieste (Hines et al., 1997; Faganeli and Ogrinc, 2009).

150   ## 3. Methods

3.1 Sediment cores

Sediment cores collected at five sites in the northern Adriatic Sea (Fig. 1) described and geochronologically-dated in our former papers were used to assess stratigraphic changes in the proportion of specimens lined with pyrite. Two sites are located at the Po prodelta (Po 3 and Po 4 at 21 m, Tomašových et al., 2018), one site in the northern Gulf of Trieste, in the

155   Bay of Panzano at 12 m at the Isonzo prodelta (Gallmetzer et al., 2017; Tomašových et al., 2017), one site in the southern Gulf of Trieste off Piran at 23 m (Mautner et al., 2018; Tomašových et al., 2019), and one site on the southern tip of Istria at Brijuni at 44 m (Schnedl et al., 2018). Sediment cores collected in 2013 are ~1.5 m long and were initially split into 2 cm-thick increments in the upper 20 cm and into 5 cm-thick increments below. The core diameter was 9 cm at the site Brijuni and 16 cm at sites Po, Panzano, and Piran. All increments were sieved with 1 mm and, with some exceptions (at Piran), all

160   individuals of *Varicorbula gibba* were picked from residues. At Piran, the increments between 10 to 35 cm were split into quarters and increments between 35 to 45 cm were split to half owing to high shell abundance (Gallmetzer et al., 2019)

     Although these sites are located at similar water depths, they differ in their proximity to clastic input from rivers, grain size, net sedimentation rate, sediment organic enrichment and iron content. Stratigraphic profiles in grain size and in concentrations of $CaCO_3$, TOC and TN, and Fe concentrations (in 63 μm sediment faction, documented in Gallmetzer et al.,

165   2017; Mautner et al., 2018; Schnedl et al., 2018) show that the three prodelta sites are exclusively muddy and rich in iron (~3%) whereas the two locations off Istria are sandy, iron-poor (1-2%), and rich in carbonate skeletal material (molluscs, echinoderms, bryozoans, coralline algae) (Fig. 2). The two Po cores are characterized by high sedimentation rate (1-2 cm/y), the Panzano core was deposited under intermediate sedimentation rate (0.2-0.4 cm/y), and the Piran and Brijuni sites are sediment-starved (<0.01 cm/y). The thickness of the surface well-mixed layer, based on homogeneity of shell ages (amino

170   acid racemization calibrated by ^{14}C) and the vertical extent of uniform or irregular segments of profiles in ^{210}Pb excess (data described by Gallmetzer et al., 2017, 2019; Tomašových et al., 2017, 2018, 2019), is ~16-20 cm at Po and at Brijuni, 6 cm at Panzano, 8 cm at Piran (where a coarse skeletal shell bed occurs at 8-35 cm below the seafloor), and 20 cm at Brijuni (where a sandy mud overlies a coarse bryozoan-rich molluscan muddy sand). Owing to geographic differences in net sedimentation rates, these estimates apply to the depths that are fully-mixed at decadal (Po and Panzano) and millennial time scales (Piran

175   and Brijuni). Some incomplete mixing also occurs below these depths (Tomašových et al., 2018) . The cores at Piran and Brijuni are mixed by bioturbation but can be subdivided to units deposited during the transgressive systems tract (TST), maximum flooding zone (MFZ), highstand systems tract (HST, prior to the 20th century), and the uppermost zones that contain a mixture of late-highstand and 20th century sediments (Fig. 2). The core at Panzano captures about 500 years and the 20th century sediments occur in the upper 35 cm. The cores at Po consist of sediments deposited during the early and the late

180   20th century (and the earliest 21st century), as described by Gallmetzer et al. (2017), Tomašových et al. (2018, 2019), Mautner et al. (2018), and Schnedl et al. (2018).

     We target specimens of the bivalve *V. gibba* because this species tends to be common in all cores and its intrinsic attributes with tightly-closed valves can favor the formation of reduced microniches (Fig. 3). The shells of this species consist of two unequal-sized valves that are formed by an outer (with a cross-lamellar structure) and an inner (with a cross-

185   lamellar and complex cross-lamellar structure) layer (Fig. 3A). Both valves possess one or more conspicuous internal, 10-100 μm-thick conchiolin layers (Fig. 3B-C), with embedded aragonite nodules (< 5 μm) (Lewy and Samtleben, 1979; Kardon, 1998). The internal conchiolin layer in the right valve terminates on the internal surface in a groove between the pallial line and the ventral margin (Fig. 3). First, the margin of the left valve is pressed on this edge of the conchiolin layer in the groove so that the left valve is almost perpendicular relative to the right valve. Second, the external periostracum of the

190   left valve overlaps with the ventral external margin of the right valve. These traits allow a tight closure of articulated valves. Although the conchiolin in the internal layers is more refractory and insoluble (Krampitz et al., 1983) than labile organics initially lining the interior of valves, the internal conchiolin layers within valves can be also prone to the decay under reducing conditions.

195   **3.2 Age distributions of pyrite-lined valves**

     D/L values and concentrations of eight amino acids (aspartic, glutamic, serine, alanine, valine, phenylalanine, isoleucine, and leucine) in valves of *V. gibba* were measured at Northern Arizona University using reverse-phase high-pressure liquid chromatography (RP-HPLC) and the procedures of Kaufman and Manley (1998). These data were measured in 252 valves

from Po 3, in 243 valves from Po 4, in 311 valves from Panzano, and in 232 valves from Piran, and were presented with age

200   calibrations of aspartic acid D/L by ^{14}C-dated valves by Tomašových et al. (2017, 2018) and Mautner et al. (2018). To
constrain the rate and the location of pyrite formation on the basis of postmortem age data, we evaluated (1) whether valves
of the same postmortem age (binned to 10 years at Po stations and to 50 years at Panzano), with and without pyrite linings,
differ in their mean stratigraphic depth or whether pyrite-lined valves are located deeper, (2) whether the rate of valve-loss
from the mixed layer (by burial or by disintegration) differs between valves with and without pyrite linings, and 3) whether

205   valves of the same age with and without pyrite linings differ in their content of amino acids. We assess the differences in
depth and age between valves with and without pyrite by comparing their mean values and 95% bootstrapped confidence
intervals. We estimate loss rates of valves from the mixed layer by fitting age distributions of valves with and without pyrite
linings from Po and Panzano to a simple model with temporally-constant loss rate that can be well-fitted by the exponential
distribution (disintegration-burial model) and to a more complex model where loss rate declines with postmortem age at

210   some sequestration rate and the resulting age distributions are heavy-tailed, typically caused by exhumation of older valves
to sediment surface (Tomašových et al., 2014). We use the Akaike Information Criterion corrected for small sample size to
assess the relative fit of these two models. The higher support for the disintegration-burial model can indicate that the both
types of valves undergo a simple, temporally-constant loss from the mixed layer. We use independent estimates of net
sedimentation rate based on ^{210}Pb data to assess whether this loss-rate parameter corresponds to disintegration or burial. The

215   higher support for the more complex model could indicate that pyrite-lined valves were exhumed from deeper zones to the
mixed layer.

3.3 Taphonomic scoring

To assess the nature and types of pyrite linings, we evaluated preservation of all specimens of *V. gibba* at light-microscope

220   scale at 10-20x magnification. We investigated several specimens with scanning electron microscope (SEM) and with
backscattered electrons (BSE), using electron probe microanalyzer at 100-1,000x magnification. The chemical composition
of pyrite and iron oxides was validated with energy-dispersive X-ray spectroscopy. All valves of *V. gibba* that were dated by
amino-acid racemization at four sites (Po 3, Po 4, Panzano M28, and Piran M53) were scored. At Po 3 (replicate cores M12,
M13 and M14, Po 4 (cores M20 and M21), Panzano (cores M28 and M29), all additional specimens were scored under a

225   light microscope. At Brijuni, all specimens of *V. gibba* from every second increment were scored. Nine alteration variables
were scored on specimens of *V. gibba* at light-microscope magnification (10-20x): (1) pyrite presence (black grains and
framboids on interior valve surfaces), (2) loss of periostracum and/or of the internal conchiolin layer (if either external
periostracum and/or internal conchiolin layer are visible, conchiolin is scored as being preserved), (3) disarticulation, (4)
internal fine-scale surface dissolution, (5) internal bioerosion (generated by algae and sponges, excluding predatory drilling),

230   (6) external encrustation, (7) intense surface wear (loss of external ornamentation), and (8) penetrative dark gray staining
(induced by nanopyritic inclusions that fill valve microporosity).

3.4 Geographic and stratigraphic differences in the frequency of pyrite-lined valves

To evaluate stratigraphic and geographic changes in preservation of *V. gibba* at the increment scale, we compute relative

235   frequencies of specimens with a given alteration relative to the total number of specimens in 4 cm (pooling 2 cm increments
in the upper 20 cm in each core) and 5 cm-thick increments at five stations. The frequency of disarticulated shells is
computed as the number of all articulated specimens in a given increment divided by the minimum number of individuals

(i.e., the sum of articulated shells plus the higher number of left or right valves). Although the estimates of disarticulation are biased upward owing to disarticulation that takes place during sieving, we assume that this bias affects all increments

240   equally. All increments were plotted and analyzed in stratigraphic analyses. However, the downcore stratigraphic profiles reflect (1) downcore changes in early-diagenetic conditions within the mixed layer driven by vertical changes in O_2 penetration and by the extent of iron and sulfate reduction and (2) chronological changes in biogeochemical processes (e.g., driven by eutrophication-induced changes in organic input and in O_2 exposure of sedimentary particles). Therefore, assuming that preservation of valves below the mixed layer is permanent, our inferences about chronological changes in preservation

245   are based on the subsets of stratigraphic profiles below the mixed layer (and on increments with more than 10 scored individuals). In analyses assessing bivariate and multivariate relationships among all alteration variables, we extracted the increments located below the mixed layer with more than 10 specimens, and measured Spearman rank correlations between per-increment frequencies of pyrite-lined valves on one hand and other types of alteration on the other hand. We use principal coordinate analysis to investigate (1) geographic differences in preservation of *V. gibba* among all sites and (2)

250   differences in preservation of *V. gibba* between the late 20th century increments (that primarily capture the main eutrophication phase) and increments that are older (corresponding to the early 20th century at the Po prodelta and the 16-19th centuries at the Isonzo prodelta) at the three prodelta sites with high sediment accumulation rates.

3.5 Relationship with ecosystem indices

255   To assess whether shell preservation responds to the ecosystem shift in the 20th century, we rank correlate the frequencies of pyrite-lined valves on one hand with several indicators of community states typical of the eutrophication phase (marked by high abundance and size of the hypoxia-tolerant bivalve *V. gibba*) on the other hand, including (1) absolute (per 0.02 m^2 and 5 cm-thick increments) and (2) proportional abundances of *V. gibba* (relative to the total molluscan abundance), (3) maximum shell size of *V. gibba* (measured by the 95th percentile of length distributions per increment), and (4) its

260   population-level biomass index based on the sum of biovolumes of all specimens that were preserved (assuming that rates of disintegration did not vary during the deposition of cores). We use the per-individual biomass-biovolume regression equation of Stanton and Powell (1985) to compute the specimen-level estimates of biomass on the basis of shell length and height of *V. gibba*. Absolute abundances of *V. gibba* at Brijuni were multiplied by a factor of 3.2 to correct for the smaller core diameter at Brijuni. Although absolute and proportional abundances are affected by between-core variability in time

265   averaging and in net sedimentation rate, trends in proportional and absolute abundance within cores can be robust because sedimentation rates remained relatively constant during the deposition of individual cores.

4. Results
4.1 Preservation of pyrite and valves at light-microscope scales

270   The preservation of *V. gibba* valves varies from well-preserved valves with periostracum (Fig. 4A-B; 4A-B) or without periostracum (Fig. 4C-D), with well-preserved pallial line and the internal conchiolin groove (pl and clg in Fig. 4), to valves with signs of fine-scale dissolution and delaminated into two distinct valve layers (originally separated by the internal conchiolin layer, Fig. 4E-F and 4G-H). This delamination is a characteristic signature of *V. gibba* preservation driven by the decay of internal conchiolin layer at all stations (Fig. 4E-H, 5C-H). The internal conchiolin layer (icl) located ventrally

275   below the pallial line can be exposed in fragments (Fig. 4I) or in delaminated valves (Fig. 4F). The interiors of valves at Po and Panzano are frequently lined by dispersed pyrite microcrystals, by individual pyrite framboids, or by aggregates of pyrite

framboids whereas pyrite-lined valves are rare at Piran and Brijuni, especially in valves with periostracum and internal conchiolin. Pyrite framboids are randomly dispersed on valve interiors (Fig. 4J-K), are arranged in filamental strings (Fig. 4L), and form continuous (Fig. 4M-N) or patchy internal linings (Fig. 4O-P). Framboids are rare on exteriors.

280   Pyrite linings can be associated with internal fine-scale dissolution and can co-occur with reddish grains of Fe oxides at all sites. However, the dissolution of valves at Po and Panzano is minor, and is still associated with some surviving portions of periostracum or conchiolin layer. Specimens from Piran and Brijuni are bored and dissolved but are rarely lined by pyrite framboids (Fig. 5). In contrast to pristine valves without any framboids on interiors (Fig. 6A), the pyrite linings can be detected in thin sections as linings formed by framboids dispersed on interior valve surfaces (black grains in Fig. 6B-D)

285   and in the conchiolin layer (Fig. 6E). Valves at Piran and Brijuni contain dispersed framboids that are mainly concentrated in borings or are associated with secondary sediment fillings of borings (Fig. 6F). Some relatively pristine valves from Po and Panzano show a blueish-colored staining on the interior and exterior, still with well-preserved external ornamentation (Fig. 4Q-T). In contrast, gray-stained valves at Piran and Brijuni are worn, degraded by bioerosion, and affected by internal encrustation (Fig. 5). In thin sections, macroborings produced by sponges are very rare in valves from Po and Panzano, and

290   bioerosion is primarily limited to simple borings that are few microns thick. In contrast, valves from Piran and Brijuni exhibit dense borings (Fig. 6F).

4.2 Preservation of pyrite at 100-1,000x magnification

On one hand, BSE images show that pyrite framboids preserved on the interiors of well-preserved valves vary in shape, size

295   (5-10 μm) and packing, ranging from densely- and regularly-packed microcrystals within spherical framboids up to loosely and irregularly-packed microcrystals within irregularly-shaped framboids (Fig. 7A-G). They coalesce into continuous agglomerations at some places. Framboids also partly fill pores between aragonite nodules (arrows in Fig. 7I) within the conchiolin layer (that is ~10-100 μm thick) where they can be partly altered by Fe oxide rims (Fig. 7H-I). Larger euhedral pyrite crystals were not observed on valve interiors. At Piran and Brijuni, pyrite framboids located in borings (secondary

300   linings) occur within strongly bored and stained valves (Fig. 7L). On the other hand, in addition to framboidal pyrite that forms primary or secondary linings, another type of pyrite preservation can be detected at high magnification and is characteristic of stained valves. The valves that are stained show disseminated or dispersed inclusions of nanopyrite (< 1 μm) in BSE images. These inclusions are located in nanoscale-dissolution pits and microborings located in the inner or the outer layer; they are not located on valve surfaces or within the conchiolin layer (Fig. 7J-L).

305   SEM images show that pyrite framboids on surfaces of non-bored or unworn valves at Po and Isonzo prodeltas are attached to the original interior surface (primary linings). Dispersed microcrystals uniformly cover inner, well-preserved and smooth surface or fill irregularities close to the groove around the termination of the internal conchiolin layers (Fig. 8A-D). Dispersed microcrystals and subspherical to spherical framboids consisting of microcrystals co-occur together and can be distributed across the whole interior surfaces in clusters (Fig. 8E), in strings (Fig. 8F) and locally co-occur with Fe oxides

310   and gypsum (Fig. 8F). Pristine valves show no or weak bioerosion by larger borers (sponges), although they can be penetrated by simple non-branching borings with micrometric diameters. In contrast, pyrite framboids are rare on interiors of valves that are affected by dense borings produced by sponges, forming complicated galleries, with or without sediment infill (Fig. 8G-H). SEM and BSE observations show that pyrite framboids directly attached to interior surfaces of well-preserved and weakly-bored valves represent primary linings, whereas pyrite framboids occurring on highly-altered valves

315   are located in borings and represented secondary linings.

4.3 Age and depth distributions

Age distributions of valves with and without pyrite linings show right-skewed shapes in the mixed layer at prodelta sites, with median age equal to 7-10 (without pyrite) and 7-18 years (with pyrite linings) at Po (in the upper 20 cm) and to 11

320   (without pyrite) and 15 years (with pyrite linings) at Panzano (in the upper 6 cm), respectively (Fig. 9A-F). They are dominated by recentmost cohorts younger than 10 years. In the mixed layer, valves with and without pyrite linings exhibit the same distribution shape well-fitted by the exponential distribution, with similar loss-rate parameters within each site (Fig. 9A-F). Therefore, the model with constant burial and disintegration outperforms or is equally efficient than more complex sequestration models both for valves with and without pyrite in the mixed layer at Po and Panzano (black lines in Fig. 9A-F,

325   Table A1). The time to valve loss from the mixed layer is similar to ^{210}Pb-based estimates of sediment accumulation (1-2 cm/y at Po and 0.2 cm at Panzano), indicating that loss rates primarily correspond to burial rates. The pyrite framboids thus form at yearly scales and valves with and without pyrite linings are buried below the mixed layer at comparable rates. Age distributions of *V. gibba* valves without pyrite linings in the mixed layer at Piran are right-skewed but fat-tailed and contain valves that are older than 1,000 years (median age =1,100 years; only one 140 years-old valve was lined by pyrite, figure not

330   shown). At the scale of the whole cores, median age of pyrite-lined valves and valves without pyrite are also comparable at Po (27 and 33 years with and without pyrite, respectively) and Panzano (100 and 124 years with and without pyrite linings, respectively) (Fig. 9G-L). However, the whole-core age distributions of valves show signs of multimodality, and the frequency with pyrite-lined valves peaks at 1986 AD at Po and at 1963 AD at Panzano. Equally-old pyrite-lined valves and valves without pyrite tend to be located at similar depths within the mixed layer (Fig. 9M-O). The mean depth of valves

335   younger than 10 years is 20 cm for specimens both with and without pyrite at Po, and pyrite-lined valves are located deeper (at 60 cm) than valves without pyrite (at 40 cm) in the 20-year cohort.

4.4 Preservation of pyrite-lined valves relative to other types of alteration

Controlling for postmortem age, valves lined by pyrite contain higher concentrations of amino acids than valves without

340   pyrite at Po and Panzano (Fig. 10). Median concentrations of amino acids in valves with pyrite linings typically exceed those in valves without pyrite within the same age cohort (Fig. 10A-C), and the log-log relationship between postmortem age and amino acid concentrations show that intercepts of valves lined by pyrite exceed intercepts of valves without pyrite by a factor of ~2 (Fig. 10D-F). Qualitative observations show that pyrite at Po and Panzano *V. gibba* preferentially formed both within valves and on internal surfaces in articulated shells, and all articulated shells from Po and Panzano that were opened

345   had pyrite on valve interiors. At the scale of individual specimens, pyrite-lined valves possess some relics of periostracum or conchiolin layer more frequently than valves without pyrite linings (Fig. 10G-I). At the scale of increments, the relations between preservation of pyrite-lined valves and other types of alteration exhibit three patterns. First, per-increment frequencies of pyrite-lined valves rank correlate *negatively* with the frequencies of disarticulated shells (Fig. 11A), with the frequencies of valves with some relics of periostracum or conchiolin layer (Fig. 11B-C), and with the frequencies of

350   bioerosion, staining, and encrustation (Fig. 11D-F). Second, the rank correlation between per-increment frequencies of pyrite-lined valves and frequencies of dissolved valves across all sites is low, but partitioning the sites by high and low sedimentation rate (with frequent and rare pyrite, respectively), frequencies of pyrite-lined valves correlate with frequencies of dissolved valves positively at Po and Panzano and negatively at Piran and Brijuni (Fig. 11G). Third, with the exception of pyrite linings, all other types of alterations covary *positively* (Fig. 11H-O). These correlations are determined by the among-

355 site gradient in sedimentation rate (associated with the gradient in grain size and carbonate content): *V. gibba* valves at sites with high sedimentation are well preserved and rarely bored, encrusted, abraded or stained (Fig.4). In contrast, *V. gibba* valves at sites with slow sedimentation show a broader range of preservational signatures, with high abundance of bored, encrusted, worn and stained specimens (Fig. 5). Valves with periostracum or conchiolin layer are abundant at Po and Panzano (with 10-80% specimens per increment), whereas such specimens are extremely rare at Piran and Brijuni, with

360 almost 100% specimens without periostracum. Principal coordinate analysis of increments from all sites shows a major separation in preservation of *V. gibba* among increments deposited at low and high sedimentation rate (Fig. 12A-B). The first PCO axis correlates negatively with frequencies of pyrite linings and positively with all other alteration variables (with the exception of fine-scale dissolution).

4.5 Stratigraphic trends in the frequency of pyrite-lined valves within the mixed layer

365

The frequency of pyrite-lined valves within the mixed layer is highly irregular at Po prodelta. Valves with pyrite increase in abundance below the mixed layer at the scale of 10 cm increments from 15-24% at 10-20 cm to 35-50% at Po 4. There is no clear downcore trend within this interval at Po 3, and the uppermost increments already contain 40% of pyrite-lined valves. The abundances of pyrite-lined valves within the mixed layer increase from 10-20% at 4-8 cm to 55-70% at 12-20 cm at

370 Panzano, with the increase coinciding with the base of the ^{210}Pb-defined mixed layer at 6 cm. At Piran and Brijuni, the frequencies within the mixed layer also do not show any obvious trend.

4.6 Stratigraphic trends in the frequency of pyrite-lined valves below the mixed layer

At sites with high sedimentation rate, the frequency of pyrite-lined valves is highest (50-80%) in increments with the

375 smallest bioturbation and the highest organic content (at 20-80 cm at Po and at 8-20 cm at Panzano, Fig. 12D), coinciding with the late 20th century eutrophication and hypoxia. This maximum declines downcore to 20% at Po prodelta (at 80-150 cm) and to 30-40% at Panzano (at 20-150 cm) in units deposited prior to the late 20th century. The frequencies of pyrite-lined valves do not change markedly at sites with slow sedimentation and are typically less than 20% at Piran and Brijuni. The frequencies of pyrite-lined valves at Piran and Brijuni further decline when they are limited to valves not affected by

380 bioerosion (black circles in Fig. 12D). Focusing on these sites with high sedimentation rate, PCO shows consistent separation between the latest HST and the late 20th century increments (Fig. 12C), reflecting the chronological increase in the frequency of pyrite linings. This within-core increase in the frequency of pyrite linings is coupled with an upcore increase in the frequency of valves without the periostracum (Fig. 13A). The frequencies of articulated valves and valves with fine-scale dissolution also increase upcore (Fig. 13B-C). At sites with slower sedimentation and coarser, carbonate-rich sediments, the

385 frequency of pyrite-lined valves remains constant upcore (<20%). The frequency of pyrite-lined valves not affected by borers is <10%. The frequency of bored specimens gradually increases from 20-30% in the lower (transgressive systems tract) increments to 70-80% in the upper (late-highstand systems tract) increments at Piran (Fig. 13). In contrast, the frequency of bored specimens gradually declines from 90-100% in the lower (transgressive systems tract) incremens to ~40% in the upper highstand increments at Brijuni (Fig. 13).

390

4.8 Relationship between pyrite-linings and ecosystem indices

Per-increment maximum shell size of *V. gibba* correlates positively with its proportional abundance ($r = 0.46$, $p < 0.0001$) and absolute abundance ($r = 0.46$, $p < 0.0001$) across all sites. Proportional abundance of *V. gibba* per increment correlate positively but rather weakly with the per-increment frequency of valves lined with pyrite framboids (r [prop. abundance] =

395   0.21, $p = 0.016$). Absolute abundance does not correlate with the per-increment frequency of pyrite-lined valves across all sites (r [abs. abundance] = -0.001, $p = 0.99$, Fig. 14). However, in contrast to regional-scale relationships that are affected by between-core differences in time averaging, the positive relationships between proportional abundance and the frequency of pyrite-lined valves are stronger at the scale of individual sites at Po (r [Po 3] = 0.61, $p = 0.0015$, r [Po 4] = 0.6, $p = 0.003$, r [Po pooled] = 0.56, $p < 0.0001$). Similarly, the relationships between absolute abundance and the frequency of pyrite-lined

400   valves are stronger and positive at the scale of individual sites at Po (r [Po 3] = 0.47, $p = 0.02$, r [Po 4] = 0.5, $p = 0.014$, r [Po pooled] = 0.38, $p = 0.008$) and also at Panzano ($r = 0.26$, $p = 0.04$).

V. gibba maximum shell size and biomass per increment correlate moderately positively with the per-increment frequency of pyrite-lined valves across all sites (r [size] = 0.54, $p < 0.0001$; r [biomass] = 0.51, $p < 0.0001$). The relationships between maximum shell size of *V. gibba* and the frequency of pyrite linings are also significantly positive at the

405   scale of individual cores at sites with high sedimentation rate (r [Po 3] = 0.65, p = 0.0007, r [Po 4] = 0.49, $p = 0.017$, r [Po pooled] = 0.61, $p < 0.0001$, r [Panzano] = 0.46, $p = 0.0002$, r [Piran] = 0.55, $p = 0.16$, r [Brijuni] = 0.11, $p = 0.71$). Similarly, the relationships between biomass and the frequency of pyrite linings are significantly positive at sites with high sedimentation rate (r [Po 3] = 0.73, $p < 0.0001$, r [Po 4] = 0.6, $p = 0.003$, r [Po pooled] = 0.63, $p < 0.0001$, r [Panzano] = 0.47, $p = 0.00018$, r [Piran] = 0.36, $p = 0.38$, r [Brijuni] = 0.22, $p = 0.36$). Within-core stratigraphic series at Po and Panzano

410   show autocorrelation in the frequency of pyrite-lined valves and in abundance, biomass and maximum shell size at lag 1 (stratigraphic series at Brijuni and Piran do not show autocorrelation in these traits). Although differencing the stratigraphic series to remove autocorrelation reduces the strength of the bivariate relationships, rank correlations between the frequency of pyrite-lined valves on one hand and maximum size and biomass of *V. gibba* on the other hand remain significantly positive at Panzano (r [size] = 0.32, $p = 0.017$; r [biomass] = 0.34, $p = 0.02$) and of borderline significance at Po if

415   increments from Po3 and Po4 are pooled (r [size] = 0.3, $p = 0.047$; r [biomass] = 0.28, $p = 0.033$).

5. Discussion

5.1 Effects of net sedimentation rate on preservation of pyrite linings

420   Our observation that the pyrite-lined valves are preserved at high abundance in the subsurface stratigraphic record at Po and Isonzo prodeltas whereas they are infrequent at Piran and Brijuni indicates that the condition for their permanent sequestration below the mixed layer is enhanced when net sedimentation rate is high. Some pyrite framboids on valves at sites with slow sedimentation probably represent secondary linings because they directly occur within borings in heavily-bored valves (i.e., the difference between frequencies of pyrite linings in all and non-bored valves is large at Brijuni, Fig.

425   12D). This preservation contrasts with well-preserved pyrite-lined valves at sites with high sedimentation where exclusion of bored valves does not reduce their frequency (i.e., the difference between frequencies of pyrite linings in all and non-bored valves is small at Po and Panzano, Fig. 12D). The preservation of primary pyrite linings is thus largely limited to sites with high sedimentation rate (> 0.2 cm/y).

First, larger grain size and sediment porosity of coarse-grained sediments enhance advective pore-water fluxes
430   driven by bottom currents, hydraulic sediment reworking, or by bioirrigation (Taylor et al., 2003; Mermillod-Blondin, 2011),
promoting higher exposure of organics within shells to O_2 and stronger iron recycling (Aller, 1994) relative to fine-grained
sediments where pore water fluxes are dominated by diffusion (Mermillod-Blondin and Rosenberg, 2006; Meysman et al.,
2006). Such conditions can inhibit the initial formation of reduced micronices. Second, the lower concentrations of iron in
sediments can reduce the probability of initial pyritization at coarse-grained sites rich in carbonate sediments even in reduced
435   micronices, with H_2S diffusing away from the decay sites (Raiswell et al., 1993; Allen, 2002). Third, at sites with slow
sedimentation rates (~0.01 cm/y) and coarse and permeable sediments less rich in iron and organic carbon, regardless of
bioturbation, valves can be exposed to O_2 in the mixed layer for longer, leading to intense alteration of valves by borers,
encrusters, or by pore waters that tend to be undersaturated with respect to aragonite in the upper 10-20 cm at the Po prodelta
(Hammond et al. 1999) and in the Gulf of Trieste (Ogrinc and Faganeli, 2003). This effect will minimize both the formation
440   of reduced micronices and their susceptibility to reoxidation, and is supported by higher levels of bioerosion, encrustation,
ornamentation loss and staining at Piran and Brijuni than at coarse-grained sites with high sedimentation rates (Fig. 11-12).
Pyrite linings that initially formed in micronices will thus not survive recycling driven by bioturbation or by physical
mixing of coarse-grained deposits accumulated under a very slow sedimentation rate (~0.01 cm/y). In contrast to very low
frequency of pyrite-lined valves at sites with low sedimentation rate, frequency of valves stained by nanopyritic inclusions is
445   higher at these sites, probably reflecting long (millennial-scale) subsurface exposure of less reactive iron-bearing minerals
(relative to highly reactive iron oxide/oxyhydroxides) to sulfidic conditions (Raiswell and Canfield, 1996). Low
sedimentation rates associated with coarse-grained sediments thus exacerbate not only residence time of skeletal remains in
the shallowest sediment zones but also their net exposure to O_2. Higher recycling of organic carbon, nitrogen and sulfur at
sites with slow sedimentation in the northern Adriatic Sea is supported by pore-water biogeochemical profiles that show
450   their higher burial efficiencies at the Po prodelta relative to sites with slower sedimentation in the NW Adriatic Sea
(Giordani et al., 1992, 2002; Hammond et al., 1999). Similarly, recycling efficiency of organic carbon and nitrogen is about
85% at Piran and in the central parts of the Gulf of Trieste and less at proximal deltaic locations off the Isonzo prodelta
(Faganeli and Ogrinc, 2009).

5.2 Pyrite-lined valves in subsurface zones as a signature of short exposure to O_2 and permanent sequestration

The preferential occurrence of pyrite linings in valves with periostracum and with higher concentrations of amino acids and
the negative correlation of pyrite-lined valves with the frequencies of other types of alteration at the scale of increments
indicate that pyrite framboids formed soon after, or concurrent with, the decay of tissues of *V. gibba* and associated microbes
(framboids arranged in filaments or strings in Fig. 4L or 6F resemble bacterial relicts, Westall, 1999; Wilson and Taylor,
460   2017). Two steps are necessary for preservation of pyrite-linings in the subsurface stratigraphic record, including their initial
formation in reduced micronices and (2) the subsequent lack of their reoxidation.

(1) The early formation of concentrations of pyrite framboids that cluster on valve surfaces requires that the labile
organics within shells do not decay or are not scavenged under aerobic conditions, that the degradation of tissues and
associated microbial coatings proceeds by sulfate reduction, and that sediment is rich in iron so that sulfides remain confined
465   to the decay location (Fisher and Hudson, 1987; Raiswell et al., 1993; Schiffbauer et al., 2014). Such conditions can occur
under the decay of reactive organics in reducing conditions in non-sulfidic, iron-dominated pore-water zones (Berner, 1969;
Briggs et al., 1996; Allen, 2002; Stockdale et al., 2010). These early-sequestration conditions can be attained (i) when
freshly-dead shells are episodically buried under a deposition of new sediment sourced by river floods or storms and can

decay in reducing conditions beyond the reah of burrowers (Allison, 1988; Brett et al., 2012a, b; Schiffbauer et al., 2014),
470 (ii) when biomass of decaying organisms is tightly enclosed as in shells or skeletal pores (as in *V. gibba*) or skeletal pores,
generating reducing microenvironments (Jorgensen, 1977; Thomsen Vorren, 1984), and/or (iii) when the oxygen penetration
depth is permanently or seasonally shallow in organic-rich and poorly-permeable fine-grained sediments (e.g., when the
oxic-anoxic interface redoxcline shallows seasonally owing to higher sediment oxygen demand driven by organic
enrichment from phytoplankton blooms, mucilages or mass mortality). The first scenario with obrution is frequently invoked
475 in the deep-time stratigraphic record because it explains the short exposure of organic remains to O_2 and their rapid
sequestration below the mixed layer (Brett et al., 2012a). Distinct layers deposited by major decadal floods preserved in
cores at Po prodelta (Tesi et al., 2012; Tomašových et al., 2018) may have triggered episodic burial of benthic communities,
but similar flood-event layers were not detected at Panzano. However, (i) equally-old valves with and without pyrite linings
occur at similar depths and (ii) age distributions of pyrite-lined valves and valves without pyrite are similar, conforming to
480 the same disintegration-burial model, indicating that valves with and without pyrite were buried below the mixed layer at the
same rate. The young age of pyrite-lined valves and their high abundance in the uppermost zones of the mixed layer also
indicate that they do not represent transient valves that were just recently exhumed from deeper zones. The pyrite framboids
thus did not preferentially form within valves that were deeper in sediments as predicted by the obrution scenario and rather
precipitated in near-surface sediment levels naturally inhabited by *V. gibba*.

485 Several lines of evidence rather indicate that the second and the third scenarios are important: the initial phase of
pyrite precipitation occurred in reduced microniches (within shells) in near-surface muddy sediments with iron-dominated
pore waters and that the limited O_2 penetration (and temporary shallowing of the redoxcline under seasonally-higher oxygen
demand of sediments) enhanced the formation of reducing microniches. First, muddy sediments are on average oxygenated
to less than 1-2 cm in the northern Adriatic Sea (Epping and Helder, 1997; Moodley et al., 1998, 2000), and zones with high
490 concentrations of dissolved iron tend be limited to the uppermost 5 cm in the NW Adriatic Sea (Hammond et al., 1999) and
in the Gulf of Trieste (Faganeli and Ogrinc, 2009). In contrast, sandy sediments exhibit stronger bioirrigation and a thicker
extent of ferruginous conditions in the upper 20 cm (Faganeli and Ogrinc, 2009). Second, qualitative observations indicate
that pyrite linings are very rare in valves of *Nucula* that co-occur with pyrite-lined *V. gibba* valves, and pyrite linings occur
rarely in apertures of gastropods. Therefore, tightly-articulated shells of *V. gibba* with internal conchiolin layers can be
495 intrinsically susceptible to the formation of reducing conditions. Third, the uppermost sediments become oxygen-depleted
during late-summer mucilage, hypoxic and mass mortality events in the northern Adriatic Sea (Stachowitsch, 1984), and the
pyrite formation and the formation of reduced microniches was thus probably further enhanced when the oxic-anoxic
interface seasonally moved to the sediment-water interface during late summer (Stachowitsch, 1984; Cermelj et al., 2001).

(2) Most of the sulfide is re-oxidized in environments with bioirrigation and sediment mixing (Canfield et al., 1993;
500 Thamdrup et al., 1994a). Reduced conditions with pyrite linings within shells or burrows thus will be transient when
sedimentation rate is low and/or when bioirrigation and sediment exhumation by burrowers oxidize such microniches
(Bertics and Ziebis, 2010). The positive relation between pyrite and fine-scale dissolution, and transformation of some pyrite
grains to iron oxides and gypsum indicates that some pyrite-lined valves at Po or Panzano were briefly exposed to
oxygenated pore waters and were partly dissolved by sulfuric acid (Cai et al., 2006; Pirlet et al., 2010; Hu et al., 2011).
505 However, this reoxygenation did not erase the pyrite linings, and many valves at Po and Panzano were still buried at
sufficiently high rate relative to the time scale of pyrite oxidation and shell dissolution (ultimately driven by mixing and
bioirrigation) so that a significant subset of pyrite-lined valves survived into the subsurface record. The conditions that
ultimately allow the transit of reduced microniches formed by pyrite-lined shells at sites with high sedimentation rate into the
subsurface stratigraphic record can occur (i) when the frequency of hypoxic or mucilage events is high, leading to periodic

510 sediment organic enrichment and high oxygen demand of sediments, thus perpetually reducing the extent of O_2 sediment penetration, and/or (ii) when recovery of infaunal communities in the wake of anoxic or hypoxic events in environments affected by eutrophication (as in the northern Adriatic Sea) is slow and in hysteresis (Kemp et al., 2009; Borja et al., 2010; Duarte et al., 2015). Depending on the frequency and duration of sediment organic enrichment, two preservation scenarios can be envisioned (Fig. 15): (i) If the frequency of anoxic or hypoxic events is low and benthic communities rapidly recover,

515 articulated shells will disarticulate and disintegrate when exposed to scavengers, borers and degradation of organics in TAZ. For example, maceration of the conchiolin layer triggers delamination of valves into inner and outer layers (Fig. 3E-H). In such conditions, O_2 penetration and the thickness of the ferruginous suboxic zone will increase (van de Velde and Meysman, 2016), and the thickness of the aerobic zone and the whole mixed layer will increase (Fig. 15A). Pyrite framboids will not nucleate on valves anymore if the labile biomass and microbes coating the decaying tissues were degraded during the earlier

520 phase of decomposition. Therefore, even when sedimentation rate is relatively high and associated with bacterial sulfate reduction in microniches surrounded by iron-dominated pore waters, bioirrigation will catch up with pyrite-lined shells prior to their deep burial and thus inhibit their subsurface sequestration by oxidation. (ii) If the frequency of hypoxic events is high relative to the recovery time of the burrowing community, some subset of pyrite-lined shells can remain preserved if recovery of bioirrigation-inducing burrowers is slow and O_2 penetration depths remains close to the sediment-water interface

525 (Fig. 15B). These conditions with reduced bioturbation and limited iron recycling are typical of oxygen-depleted or strongly-eutrophied environments (Karlson et al., 2007; Lehtoranta et al., 2009). Although the present-day estimates of the mixed-layer depth in the northern Adriatic Sea do not indicate any apparent limitation on bioturbation (see below), we suggest that such conditions also characterized benthic habitats with fine-grained sedimentation in the northern Adriatic Sea in the late 20th century. If the nutrient-fueled eutrophication or other sources of sediment organic enrichment lead to permanent oxygen-

530 depletion and to sulfidic sediments at the sediment-water interface (and the formation of dead-zones), the concentrations of pyrite framboids within shells or within intra-skeletal pores will be limited by iron availability, and most pyrite will be disseminated rather than clustered.

5.3 Temporal changes in bioturbation generate stratigraphic trends in frequency of pyrite-lined valves

535 Within-core trends in the frequency of pyrite-lined valves at prodelta sites and the modality of whole-core age distributions of pyrite-lined valves hint to chronological changes in the preservation of pyrite linings. First, in addition to a general feature of the whole-core age distributions dominated by valves younger than 10 years, generated under active input of new dead shells into the mixed layer, older modes in these distributions are indicative about temporal changes in conditions that favored or inhibited the preservation of pyrite linings. At Po, pyrite-lined valves show a secondary mode at ~30-50 years that

540 is formed by cohorts from the late 20th century, and most valves older than ~100 years do not have pyrite linings (Fig. 9E-F). Similarly, at Panzano, pyrite-lined valves form a mode that is represented by cohorts from the late 20th century (Fig 9G-H). Second, the stratigraphic increase in the frequency of pyrite-lined valves and multivariate segregation in preservation of *V. gibba* valves between the early and the late 20th century increments at Po and Panzano (below the mixed layer) indicate that O_2 exposure of shells in the mixed layer was longer prior to and during the early 20th century than during the late 20th

545 century. Any effects on early diagenetic pathways determined by changes in grain size can be excluded because sediment grain size remains constant downcore at Po and Panzano. Although paleoecological records of foraminifers and dinoflagellates indicate that eutrophication affects the northern Adriatic Sea ecosystems since the 19th century (Barmawidjaja et al. 1995; Sangiorgi and Donders 2004), a main shift in the composition of macrobenthic communities and size of the bivalve *V. gibba* occurs at the same stratigraphic levels where pyrite linings increase in frequency, i.e., at 80-90 cm at Po and

550 at 12-20 cm Panzano stations (Tomašových et al., 2018, 2020). These levels correspond to the mid-20th century at both

prodeltas, and coincide with an increase in nutrient load and in seasonal hypoxia and mucilage frequency in the northern Adriatic Sea (Marchetti et al., 1989; Justic, 1991). Several mutually not exclusive factors probably contributed to the stratigraphic increase in the frequency of pyrite-lined valves, including (1) a temporal increase in hypoxia coupled with an increase in sediment organic enrichment, and (2) a temporal decline in sediment mixing and bioirrigation. Although the

555 initial formation of pyrite framboids in reduced microniches in near-surface sediments can naturally occur in fine-grained and poorly-permeable sediments, it was probably also enhanced by multiple processes that occurred during or in response to hypoxic events and accentuated seasonal shallowing of the oxic-anoxic sediment boundary (Middelburg and Levin, 2009): by a decline in dissolved oxygen concentrations in the overlying water column (reducing sediment penetration by O_2 although permanent anoxia underlain by sulfidic sediment can trigger iron escape from sediment, Pakhomova et al., 2007),

560 by decay of planktonic and benthic phytoplankton or mucilages that increased oxygen demand of sediments as they accumulated on the sediment-water interface (Herndl et al., 1987, 1989), or by decay of high-biomass epifaunal communities during late-summer mass mortality events (Stachowitsch, 1984; Nebelsick et al., 1997). The frequency and magnitude of all these effects probably increased in the late 20th century in the northern Adriatic Sea, thus increasing the likelihood of initiation of reducing microniches within articulated shells of bivalves (rather than being exposed to disarticulation by

565 predators or scavengers).

Regardless of initial pathways that led to the formation of pyrite linings in reduced microenvironments, hypoxic and mucilage events that are seasonal or inter-annual in frequency in the northern Adriatic Sea tend to be followed by recovery of infaunal species under oxygenated conditions (leading to iron recycling and pyrite oxidation), and oxygen depletion of near-surface sediments is thus not permanent if infaunal communities fully recover. However, seasonal anoxic or hypoxic

570 events have lasting effects on mixing and irrigation rates because benthic communities tend to recover from such events at slow rate (Bentley and Nittrouer, 1999; Solan et al., 2004) and can remain in a hysteresis state (Duarte et al., 2015). This delay, with benthic recoveries occurring over several years (Borja et al., 2010), was also observed in the northern Adriatic Sea (Stachowitsch, 1991). The decline in mixing and bioirrigation in the wake of hypoxic events (that became more frequent during the late 20th century in the northern Adriatic Sea) was probably crucial for transfer of pyrite linings into the

575 subsurface stratigraphic record, as envisioned in the scenario in Fig. 15B. The present-day bioturbation rates are thus probably lower relative to those that characterized the northern Adriatic Sea prior to the late 20th century. This inference is supported by three observations. First, the positive relation between *V. gibba* size and biomass on one hand and abundances of pyrite-lined valves on the other hand support the hypothesis that eutrophication-driven regime shift in the functioning of benthic communities in the late 20th century reduced biomixing and bioirrigation. Second, at Po and Isonzo prodeltas, the

580 late 20th century infauna is dominated by shallow-burrowing deposit- and detritus-feeders that modify surface sediments, including *Owenia fusiformis*, *Varicorbula gibba* or *Ampelisca diadema* (Occhipinti-Ambrogi et al., 2005; Solis-Weiss et al., 2007; N'Siala et al., 2008). These patterns differ from early 20th century ecological surveys (Vatova, 1949; Crema et al., 1991; Schinner, 1993; Schinner et al., 1997) and the early 20th century increments in cores (Gallmetzer et al., 2017; Tomašových et al., 2018) that indicate that pre-eutrophication benthic communities were dominated by biodiffusors such as

585 *Schizaster, Amphiura* or *Turritella*. The ophiuroid *Amphiura filiformis* (extensively reworking and irrigating sediments, Solan and Kennedy 2002; Vopel et al., 2003) or the gastropod *Turritella communis* are not abundant at prodelta sites and tend to occur at deeper sites with slower sedimentation rates in the northern Adriatic Sea in the late 20th century surveys (Chiantore et al., 2001). In contrast to *Amphiura*, the ophiuroid *Ophiura albida* that is abundant at Po stations belongs to slow biodiffusers. Third, abundant burrows of shrimps and the 16-20 cm-thick age-homogenized layer the Po stations

590 observed at the time of core sampling in 2013 at Po indicate that biomixing is apparently not limited: the thickness of the mixed layer is typical of mixed-layer thickness observed in other marine shelf environments (Teal et al., 2010). It is also not within the range of mixed-layer thickness typical of persistently-hypoxic environments on the scale of 5 cm on continental

slopes (interspersed with laminated sediments, Meadows et al. 2000; Smith et al. 2000; Levin et al. 2003). However, the estimates of the mixing depths on the basis of ^{210}Pb profiles indicated mixing depths < 10 cm in the late 20th century at Po

595   prodelta (Frignani and Langone, 1991; Frignani et al., 2005; Alvisi et al., 2006, 2009) and the thickness of the mixed layer at the Po prodelta as estimated on the basis of sediment cores probably exceeded 20 cm prior to the late 20th century (Tomašových et al., 2018). In addition to changes in sediment mixing, the nature of benthic communities indicates that irrigation was slower and that iron and sulfide recycling was less efficient in the late 20th century at Po and Isonzo prodeltas than earlier. To conclude, these observations support the hypothesis that the stratigraphic shift towards higher pyrite

600   frequency of pyrite-lined shells coincides with changes in the composition of macrobenthic communities that reduced their mixing and irrigation efficiency during the 20th century.

6. Implications for the fossil record: inferring slow and patchy bioturbation and limited residence time

The pyrite framboids lining intra-skeletal pores (originally filled with organic tissues) in well-preserved shells represent a unique indicator of slow irrigation and their permanent transfer below the oxic-anoxic sediment interface. Such conditions

605   can be produced by delayed recoveries from hypoxic events and/or by community states with low bioirrigation potential that are unable to recover anymore even when the frequency of hypoxic events returns to pre-impact levels (Steckbauer et al., 2011). In permanently-normoxic environments with intense bioturbation where most labile biomass degrades within the aerobic zone and any early pyrite is oxidized, the frequency of shells with shell-lined pyrite transferred into the permanent record will be negligible. This index can be also used to track the net O_2 exposure of skeletal remains and recycling

610   efficiency of iron and sulfides in the deep-time stratigraphic record because pyrite-lined shells represents a distinct taphonomic and diagenetic signature of fossil assemblages preserved in fine-grained sediments (Kobluk and Risk, 1977; Hudson, 1982; Bjerreskov, 1991; Underwood and Bottrell, 1994; Farrell et al., 2009; Brett et al., 2012a), especially in organisms with internal skeletal cavities that do not immediately open after their death (Hudson, 1982; Fisher, 1986; Loope and Watkins, 1989; Jin et al., 2007). On one hand, preservation of well-preserved, frequently articulated skeletal remains of

615   organisms with otherwise fragile elements, coupled with pyrite linings, is a typical taphonomic feature of assemblages preserved in fine-grained sediments in the Paleozoic (Brett et al., 2012a, b) or in the Mesozoic successions (Hudson, 1982; Fernández-López et al., 2000; Paul et al., 2008; Reolid, 2014). On the other hand, actualistic studies assessing skeletal alteration of molluscs, brachiopods or echinoderms rarely record this type of preservation in surface Holocene sediments. It is possible that the concentration of actualistic studies on the taphonomic processes in the mixed layer and on environments

620   with slow sediment accumulation rates underestimate this type of preservation. However, here, we suggest that prodelta sediments in the northern Adriatic Sea affected by the late 20th century eutrophication can represent analogue conditions that lead to preservation of well-preserved and pyrite-lined shells in the deep-time stratigraphic record. In contrast to models invoking rapid episodic burial to explain the initial sequestration of shells so that they do not disarticulate and decay under anaerobic conditions, the pathway observed in prodelta sediments in the northern Adriatic Sea probably occurs without

625   episodic burial. Although background sedimentation rates need to be sufficiently high so that the time for burial of skeletal remains is shorter the time to mix and irrigate the mixed layer, the effect of sedimentation rate is critical for minimizing the potential for reoxidation rather than for initial sequestration of shells in microniches.

7. Conclusions

630   Preservation of pyrite-lined shells as a function of rapid and permanent sequestration below the taphonomic active zone is an indicator of inefficient mixing and bioirrigation, thus documenting limited iron and sulfur recycling at sites with high

sedimentation rates in the northern Adriatic Sea. The preservation pathway that leads to primary pyrite linings and their long-term preservation is indicative of permanently-limited depths of O_2 penetration and bioirrigation that can be difficult to detect on the basis of trace fossils and ichnofabric only. Pyrite-lined valves thus represent a unique type of alteration that contrasts with other types of alteration whose incidence increases with residence time in the taphonomic active zone. We suggest that the increase in the frequency of valves with pyrite below the mixed layer at 80-90 cm at the Po prodelta and at 12-20 cm at the Isonzo prodelta represents a temporal signal of the decline in the rate of mixing and bioirrigation in muddy sediments of the northern Adriatic Sea driven by a late 20th century increase in the frequency of seasonal or inter-annual hypoxia and organic enrichment that delayed the recovery of infaunal communities. Although the rates of pyrite formation can also vary over long time scales owing to long-term changes in seawater chemistry (Leavitt et al., 2013; Algeo et al., 2015) and depend on the supply of organic matter and iron availability (Goldhaber et al., 1977; Berner and Raiswell, 1983; Berner, 1984; Berner and Westrich, 1985; Kershaw et al., 2018; Wignall et al., 2005, 2010), we hypothesize that the frequency of pyrite-lined shells (belonging to organisms that inhabit oxic sediment zones) can improve inferences about mixing and irrigation and about the net exposure time of skeletal particles to irrigation in the mixed layer.

Acknowledgments

This work was supported by the Austrian Science Fund (FWF) [grant number P24901, 2013, by the Slovak Research and Development Agency (APVV 0555-17) and by the Slovak Scientific Grant Agency (VEGA 2/0169-19). Many thanks to the captain of the sampling vessel, Jernej Sedmak, for his commitment during the sampling campaign in 2014.

References

Algeo, T. J., Luo, G. M., Song, H. Y., Lyons, T. W., and Canfield, D. E.: Reconstruction of secular variation in seawater sulfate concentrations. Biogeosciences, 12, 2131-2151, 2015.

Allen, R. E.: Role of diffusion–precipitation reactions in authigenic pyritization. Chem. Geol., 182, 461-472, 2002.

Aller, R. C.: Carbonate dissolution in nearshore terrigenous muds: the role of physical and biological reworking. J. Geol., 90, 79-95, 1982.

Aller, R. C.: Bioturbation and remineralization of sedimentary organic matter: effects of redox oscillation. Chem. Geol., 114, 331-345, 1994.

Aller, R. C., and Cochran, J. K.: The critical role of bioturbation for particle dynamics, priming potential, and organic C remineralization in marine sediments: local and basin scales. Front. Earth Sci., 7, 157, 2019.

Allison, P. A.: The role of anoxia in the decay and mineralization of proteinaceous macro-fossils. *Paleobiology*, 14, 139-154, 1988.

Alvisi, F., Frignani, M., Brunetti, M., Maugeri, M., Nanni, T., Albertazzi, S., and Ravaioli, M.: Climate vs. anthropogenic changes in North Adriatic shelf sediments influenced by freshwater runoff. Clim. Res., 31, 167-179, 2006.

Alvisi, F.: A simplified approach to evaluate sedimentary organic matter fluxes and accumulation on the NW Adriatic Shelf (Italy). Chem. Ecol., 25, 119-134, 2009.

Amorosi, A., Centineo, M.C., Dinelli, E., Lucchini, F., and Tateo, F.: Geochemical and mineralogical variations as indicators of provenance changes in Late Quaternary deposits of SE Po Plain. Sediment. Geol., 151, 273-292, 2002.

Anderson, E. P., Schiffbauer, J. D., and Xiao, S.: Taphonomic study of Ediacaran organic-walled fossils confirms the
670 importance of clay minerals and pyrite in Burgess Shale− type preservation. Geology, 39, 643-646, 2011.

Arcon, I., Ogrinc, N., Kodre, A., and Faganeli, J.: EXAFS and XANES characterization of sedimentary iron in the Gulf of Trieste (N. Adriatic). J. Synchrotron Radiat., 6, 659-660, 1999.

Barbanti, A., Bergamini, M. C., Frascari, F., Miserocchi, S., Ratta, M. and Rosso, G.: Diagenetic processes and nutrient fluxes at the sediment-water interface, Northern Adriatic Sea, Italy. Mar. Freshwater Res., 46, 55-67, 1999.

675 Bentley, S. J., and Nittrouer, C. A.: Physical and biological influences on the formation of sedimentary fabric in an oxygen-restricted depositional environment; Eckernforde Bay, southwestern Baltic Sea. Palaios, 14, 585-600, 1999.

Berner, R. A.: Migration of iron and sulfur within anaerobic sediments during early diagenesis. Am. J. Sci., 267, 19-42, 1969.

Berner, R. A., and Raiswell, R.: Burial of organic carbon and pyrite sulfur in sediments over Phanerozoic time: a new
680 theory. Geochim. Cosmochim. Ac., 47, 855-862, 1983.

Berner, R.A.: Sedimentary pyrite formation: an update. Geochim. Cosmochim. Ac., 48, 605-615, 1984.

Berner, R. A., and Westrich, J. T.: Bioturbation and the early diagenesis of carbon and sulfur. Am. J. Sci., 285, 193-206, 1985.

Bertics, V. J., and Ziebis, W.: Bioturbation and the role of microniches for sulfate reduction in coastal marine
685 sediments. Environ. Microbiol., 12, 3022-3034, 2010.

Best, M. M., and Kidwell, S. M.: Bivalve taphonomy in tropical mixed siliciclastic-carbonate settings. I. Environmental variation in shell condition. Paleobiology, 26, 80-102, 2000.

Boekschoten, G. J.: Shell borings of sessile epibiontic organisms as palaeoecological guides (with examples from the Dutch coast). Palaeogeogr. Palaeoclimatol. Palaeoecol., 2, 333-379, 1966.

690 Boyle, R. A., Dahl, T. W., Dale, A. W., Shields-Zhou, G. A., Zhu, M. Y., Brasier, M. D., Canfield, D. E., and Lenton, T. M.: Stabilization of the coupled oxygen and phosphorus cycles by the evolution of bioturbation. Nat. Geosci., 7, 671-676, 2014.

Borja, Á., Dauer, D. M., Elliott, M., and Simenstad, C. A.. Medium-and long-term recovery of estuarine and coastal ecosystems: patterns, rates and restoration effectiveness. Estuar. Coast., 33, 1249-1260, 2010.

Bjerreskov, M.: Pyrite in Silurian graptolites from Bornholm, Denmark. Lethaia, 24, 351-361, 1991.

695 Briggs, D. E. G., Bottrell, S. H., and Raiswell, R.: Pyritization of soft-bodied fossils: Beecher's Trilobite Bed, Upper Ordovician, New York State. Geology 19, 1221–1224, 1991.

Boldrin, A., Carniel, S., Giani, M., Marini, M., Aubry, F. B., Campanelli, A., Grilli, F., and Russo, A.: Effects of bora wind on physical and biogeochemical properties of stratified waters in the northern Adriatic. J. Geophys. Res.-Oceans, 114, 2009.

Borkow, P. S., and Babcock, L. E.: Turning pyrite concretions outside-in: role of biofilms in pyritization of fossils. Sedim.
700   Record, 1, 4-7, 2003.

Brett, C. E., Zambito IV, J. J., Hunda, B. R., and Schindler, E.: Mid-Paleozoic trilobite Lagerstätten: Models of
diagenetically enhanced obrution deposits. Palaios, 27, 326-345, 2012a.

Brett, C. E., Zambito IV, J. J., Schindler, E., and Becker, R. T.: Diagenetically-enhanced trilobite obrution deposits in
concretionary limestones: The paradox of "rhythmic events beds". Palaeogeogr. Palaeoclimatol. Palaeoecol., 367, 30-43,
705   2012b.

Briggs, D. E. G., Raiswell, R., Bottrell, S. H., Hatfield, D., and Bartels, C.: Controls on the pyritization of exceptionally
preserved fossils: an analysis of the Lower Devonian Hunsrück Slate of Germany. Am. J. Sci., 296, 633–663, 1996.

Brown, P. R.: Pyritization in some molluscan shells. J. Sediment. Res., 36, 1149-1152, 1996.

Brush, M. J., Giani, M., Totti, C., Testa, J. M., Faganeli, J., Ogrinc, N., Kemp, W. M., and Umani, S.F.. Eutrophication,
710   Harmful Algae, Oxygen Depletion, and Acidification. Coastal Ecosystems in Transition: A Comparative Analysis of the
Northern Adriatic and Chesapeake Bay, 75-104, 2020.

Buatois, L. A., and Mángano, M. G.: The déjà vu effect: Recurrent patterns in exploitation of ecospace, establishment of the
mixed layer, and distribution of matgrounds. Geology, 39, 1163-1166, 2011.

Buatois, L. A., Mángano, M. G., Minter, N. J., Zhou, K., Wisshak, M., Wilson, M. A., and Olea, R. A.: Quantifying
715   ecospace utilization and ecosystem engineering during the early Phanerozoic—The role of bioturbation and
bioerosion. Science Advances, 6, eabb0618, 2020.

Cai, W. J., Chen, F., Powell, E. N., Walker, S. E., Parsons-Hubbard, K. M., Staff, G. M., Wang, Y., Ashton-Alcox, K. A.,
Callender, W. R., and Brett, C. E.: Preferential dissolution of carbonate shells driven by petroleum seep activity in the Gulf
of Mexico. Earth Planet. Sc. Lett., 248, 227-243, 2006.

720   Cai, Y., Schiffbauer, J. D., Hua, H., and, Xiao, S.: Preservational modes in the Ediacaran Gaojiashan Lagerstätte:
pyritization, aluminosilicification, and carbonaceous compression. Palaeogeogr. Palaeoclimatol. Palaeoecol., 326–328, 109–
117, 2012.

Canfield, D. E., and Farquhar, J.: Animal evolution, bioturbation, and the sulfate concentration of the oceans. P. Natl. Acad.
Sci. USA, 106, 8123-8127, 2009.

725   Canfield, D. E., Thamdrup, B., and Hansen, J. W.: The anaerobic degradation of organic matter in Danish coastal sediments:
iron reduction, manganese reduction, and sulfate reduction. Geochim. Cosmochim. Ac., 57, 3867-3883, 1993.

Carstensen, J., Conley, D.J., Bonsdorff, E., Gustafsson, B. G., Hietanen, S., Janas, U., Jilbert, T., Maximov, A., Norkko, A.,
Norkko, J., and Reed, D. C.: Hypoxia in the Baltic Sea: Biogeochemical cycles, benthic fauna, and
management. AMBIO, 43, 26-36, 2014.

730   Cermelj, B., Ogrinc, N., and Faganeli, J.: Anoxic mineralization of biogenic debris in near-shore marine sediments (Gulf of
Trieste, northern Adriatic). Sci. Total. Environ., 266, 143-152, 2001.

Chiantore, M., Bedulli, D., Cattaneo-Vietti, R., Schiaparelli, S., and Albertelli, G: Long-term changes in the Mollusc–Echinoderm assemblages in the north and coastalmiddleAdriatic Sea. Atti Assoc. It. Oceanol. Limnol., 14:63–75, 2001.

Christensen, B., Vedel, A. and Kristensen, E., 2000. Carbon and nitrogen fluxes in sediment inhabited by suspension-feeding (*Nereis diversicolor*) and non-suspension-feeding (*N. virens*) polychaetes. Mar. Ecol. Prog. Ser., 192, 203-217.

Clark, G. R.; and Lutz, R. A.: Pyritization in the shells of living bivalves. Geology, 8, 268-271, 1980.

Degobbis, D., Precali, R., Ivancic, I., Smodlaka, N., Fuks, D., and Kveder, S.: Long-term changes in the northern Adriatic ecosystem related to anthropogenic eutrophication. Int. J. Environ. Pollut., 13, 495-533, 2000.

Cozzi, S., Ivančić, I., Catalano, G., Djakovac, T., and Degobbis, D.: Dynamics of the oceanographic properties during mucilage appearance in the Northern Adriatic Sea: analysis of the 1997 event in comparison to earlier events. J. Marine Syst., 50, 223-241, 2004.

Crema, R., Castelli, A., and Prevedelli, D. Long term eutrophication effects on macrofaunal communities in northern Adriatic Sea. Mar. Pollut. Bull., 22, 503-508, 1991.

Davies, D. J., Powell, E. N., and Stanton Jr, R. J.: Relative rates of shell dissolution and net sediment accumulation-a commentary: can shell beds form by the gradual accumulation of biogenic debris on the sea floor? Lethaia, 22, 207-212, 1989.

Djakovac, T., Supić, N., Aubry, F. B., Degobbis, D., and Giani, M.: Mechanisms of hypoxia frequency changes in the northern Adriatic Sea during the period 1972–2012. J. Marine Syst., 141, 179-189, 2015.

Dolenec, T., Faganeli, J., and Pirc, S.: Major, minor and trace elements in surficial sediments from the open Adriatic Sea: a regional geochemical study. Geol. Croat., 51, 59-73, 1998.

Droser, M. L., and Bottjer, D. J.: Trends in depth and extent of bioturbation in Cambrian carbonate marine environments, western United States. Geology, 16, 233-236, 1988.

Droser, M. L., Jensen, S., and Gehling, J. G.: Trace fossils and substrates of the terminal Proterozoic–Cambrian transition: implications for the record of early bilaterians and sediment mixing. P. Natl. Acad. Sci. USA, 99, 12572-12576, 2002.

Duarte, C. M., Borja, A., Carstensen, J., Elliott, M., Krause-Jensen, D., and Marbà, N.: Paradigms in the recovery of estuarine and coastal ecosystems. Estuar. Coast., 38, 1202-1212, 2015.

Elliott, M., Burdon, D., Hemingway, K. L., and Apitz, S. E.: Estuarine, coastal and marine ecosystem restoration: confusing management and science–a revision of concepts. Estuar. Coast. Shelf S., 74, 349-366, 2007.

Emery, K. O., and Rittenberg, S. C.: Early diagenesis of California basin sediments in relation to origin of oil. AAPG Bulletin, 36, 735-806, 1952.

Epping, E. H. and Helder, W.: Oxygen budgets calculated fromin situ oxygen microprofiles for Northern Adriatic sediments. Cont. Shelf Res., 17, 1737-1764, 1997.

Faganeli, J., Avčin, A., Fanuko, N., Malej, A., Turk, V., Tušnik, P., Vrišer, B., and Vuković, A.: Bottom layer anoxia in the central part of the Gulf of Trieste in the late summer of 1983. Mar. Pollut. Bull., 16, 75-78, 1985.

765   Faganeli, J., Planinc, R., Smodiš, B., Stegnar, P., and Ogorelec, B.: Marine geology of the Gulf of Trieste (northern Adriatic): geochemical aspects. Mar. Geol., 99, 93-108, 1991.

Faganeli, J., Pezdic, J., Ogorelec, B., Misic, M., and Najdek, M.: The origin of sedimentary organic matter in the Adriatic. Cont. Shelf Res., 14, 365-384, 1994.

Faganeli, J., and Ogrinc, N.: Oxic–anoxic transition of benthic fluxes from the coastal marine environment (Gulf of Trieste, 770   northern Adriatic Sea). Marine and Freshwater Research, 60, 700-711, 2009.

Farrell, Ú. C., Martin, M. J., Hagadorn, J. W., Whiteley, T., and Briggs, D. E.: Beyond Beecher's Trilobite Bed: Widespread pyritization of soft tissues in the Late Ordovician Taconic foreland basin. Geology, 37, 907-910, 2009.

Fedra, K., Ölscher, E. M., Scherübel, C., Stachowitsch, M., and Wurzian, R. S.: On the ecology of a North Adriatic benthic community: distribution, standing crop and composition of the macrobenthos. Mar. Biol., 38, 129-145, 1976.

775   Fernández-López, S. R., Duarte, L. V., and Henriques, M. H. P.: Ammonites from lumpy limestones (Lower Pliensbachian, Portugal). Taphonomic analysis and palaeoenvironmental implications. Rev. Soc. Geol. España, 13, 3-15, 2000.

Fisher, I. S. J.: Pyrite replacement of mollusc shells from the Lower Oxford Clay (Jurassic) of England. Sedimentology, 33, 575-585, 1986.

Fisher, I. S. J., and Hudson, J. D.: Pyrite formation in Jurassic shales of contrasting biofacies. Geol. Soc. Spec. Publ., 26, 69-780   78, 1987.

Frignani, M., and Langone, L.: Accumulation rates and ^{137}Cs distribution in sediments off the Po River delta and the Emilia-Romagna coast (northwestern Adriatic Sea, Italy). Cont. Shelf Res., 11, 525-542, 1991.

Frignani, M., Langone, L., Ravaioli, M., Sorgente, D., Alvisi, F., and Albertazzi, S.: Fine-sediment mass balance in the western Adriatic continental shelf over a century time scale. Marine Geology, 222, 113-133, 2005.

785   Gabbott, S. E., Xian-Guang, H., Norry, M. J., and Siveter, D. J.: Preservation of Early Cambrian animals of the Chengjiang biota. Geology, 32, 901-904, 2004.

Gallmetzer, I., Haselmair, A., Tomašových, A., Stachowitsch, M. and Zuschin, M.: Responses of molluscan communities to centuries of human impact in the northern Adriatic Sea. PLoS One, 12, e0180820, 2017.

Gehling, J. G.: Microbial mats in terminal Proterozoic siliciclastics; Ediacaran death masks. *Palaios*, *14*, 40-57, 1999.

790   Germano, J. D., Valente, R. M., Carey, D. A., and Solan, M.: The use of Sediment Profile Imaging (SPI) for environmental impact assessments and monitoring studies: lessons learned from the past four decades. Oceanography and Marine Biology: An Annual Review, 49, 235–298, 2011.

Gerwing, T. G., Cox, K., Gerwing, A. M. A., Carr-Harris, C. N., Dudas, S. E., and Juanes, F.: Depth to the apparent redox potential discontinuity (aRPD) as a parameter of interest in marine benthic habitat quality models. International Journal of 795   Sediment Research, 33, 149-156, 2018.

Giani, M., Savelli, F., Berto, D., Zangrando, V., Ćosović, B. and Vojvodić, V.: Temporal dynamics of dissolved and particulate organic carbon in the northern Adriatic Sea in relation to the mucilage events. Sci. Total. Environ., 353, 126-138, 2005.

Gibson, B. M., Schiffbauer, J. D., and Darroch, S. A.: Ediacaran-style decay experiments using mollusks and sea anemones. Palaios, 33, 185-203, 2018.

Gingras, M. K., Pemberton, S. G., Dashtgard, S., and Dafoe, L.: How fast do marine invertebrates burrow? Palaeogeogr. Palaeoclimatol. Palaeoecol., 270, 280-286, 2008.

Giordani, P., Hammond, D. E., Berelson, W. M., Montanari, G., Poletti, R., Milandri, A., Frignani, M., Langone, L., Ravaioli, M., Rovatti, G., and Rabbi, E.: Benthic fluxes and nutrient budgets for sediments in the Northern Adriatic Sea: burial and recycling efficiencies. In Marine coastal eutrophication (pp. 251-275). Elsevier, 1992.

Giordani, P., Helder, W., Koning, E., Miserocchi, S., Danovaro, R., and Malaguti, A.: Gradients of benthic–pelagic coupling and carbon budgets in the Adriatic and Northern Ionian Sea. J. Marine Syst., 33, 365-387, 2002.

Goldhaber, M. B., Aller, R. C., Cochran, J. K., Rosenfeld, J. K., Martens, C. S., and Berner, R. A.: Sulfate reduction, diffusion, and bioturbation in Long Island Sound sediments; report of the FOAM Group. Am. J. Sci., 277, 193-237, 1977.

Gougeon, R. C., Mángano, M. G., Buatois, L. A., Narbonne, G. M., and Laing, B. A.: Early Cambrian origin of the shelf sediment mixed layer. Nat. Commun., 9, 1-7, 2018.

Hines, M. E., Faganeli, J., and Planinc, R.: Sedimentary anaerobic microbial biogeochemistry in the Gulf of Trieste, northern Adriatic Sea: influences of bottom water oxygen depletion. Biogeochemistry, 39, 65-86, 1997.

Hartnett, H. E., Keil, R. G., Hedges, J. I., and Devol, A. H.: Influence of oxygen exposure time on organic carbon preservation in continental margin sediments. Nature, 391, 572-575, 1998.

Hammond, D. E., Giordani, P., Berelson, W. M., and Poletti, R.: Diagenesis of carbon and nutrients and benthic exchange in sediments of the Northern Adriatic Sea. Mar. Chem., 66, 53-79, 1999.

Herndl, G. J., Faganeli, J., Fanuko, N., Peduzzi, P., and Turk, V.: Role of bacteria in the carbon and nitrogen flow between water-column and sediment in a shallow marine bay (Bay of Piran, Northern Adriatic Sea). Mar. Ecol., 8, 221-236, 1987.

Herndl, G. J., Peduzzi, P., and Fanuko, N.: Benthic community metabolism and microbial dynamics in the Gulf of Trieste (Northern Adriatic Sea). Mar. Ecol. Prog. Ser., 53, 169-178, 1989.

Hu, X., Cai, W. J., Wang, Y., Guo, X. and Luo, S.: Geochemical environments of continental shelf-upper slope sediments in the northern Gulf of Mexico. Palaeogeogr. Palaeoclimatol. Palaeoecol., 312, 265-2772011, 2011.

Hudson, J. D.: Pyrite in ammonite-bearing shales from the Jurassic of England and Germany. Sedimentology, 29, 639-667, 1982.

Hunda, B. R., Hughes, N. C., and Flessa, K. W.: Trilobite taphonomy and temporal resolution in the Mt. Orab shale bed (Upper Ordovician, Ohio, USA). Palaios, 21, 26-45.

Jerolmack, D. J., and Sadler, P.: Transience and persistence in the depositional record of continental margins. J. Geophys. Res.: Earth, 112, 2007.

Jin, J., Zhan, R., Copper, P., and Caldwell, W. G. E.: Epipunctae and phosphatized setae in Late Ordovician plaesiomyid brachiopods from Anticosti Island, eastern Canada. J. Paleontol., 81, 666-683, 2007.

Jørgensen, B. B.: Bacterial sulfate reduction within reduced microniches of oxidized marine sediments. Mar. Biol., 41, 7-17, 1977.

Justić, D.: Hypoxic conditions in the northern Adriatic Sea: historical development and ecological significance. Geol. Soc. Spec. Publ., 58, 95-105, 1991.

Kardon, G.: Evidence from the fossil record of an antipredatory exaptation: conchiolin layers in corbulid bivalves. Evolution, 52, 68-79, 1998.

Karlson, K., Bonsdorff, E., and Rosenberg, R.: The impact of benthic macrofauna for nutrient fluxes from Baltic Sea sediments. AMBIO, 36, 161-167, 2007.

Kemp, W. M., Faganeli, J., Puskaric, S., Smith, E. M., and Boynton, W. R.: Pelagic-benthic coupling and nutrient cycling. Ecosystems at the land-sea margin: Drainage basin to coastal sea. Estuar. Coast. Shelf S., 55, 295-340, 1999.

Kemp, W. M., Testa, J. M., Conley, D. J., Gilbert, D. and Hagy, J. D.: Temporal responses of coastal hypoxia to nutrient loading and physical controls. Biogeosciences, 6, 985-3008, 2009.

Kobluk, D. R., and Risk, M. J.: Algal borings and framboidal pyrite in Upper Ordovician brachiopods. Lethaia, 10, 135-143, 1977.

Kralj, M., Lipizer, M., Čermelj, B., Celio, M., Fabbro, C., Brunetti, F., Francé, J., Mozetič, P., and Giani, M.: Hypoxia and dissolved oxygen trends in the northeastern Adriatic Sea (Gulf of Trieste). Deep-Sea Res. Pt. II, 164, 74-88, 2019.

Krampitz, G., Drolshagen, H., and Hotta, S.: Simultaneous binding of calcium and bicarbonate by conchiolin of oyster shells. Experientia, 39, 1104-1105, 1983.

Kristensen, E., Penha-Lopes, G., Delefosse, M., Valdemarsen, T., Quintana, C. O., and Banta, G. T.: What is bioturbation? The need for a precise definition for fauna in aquatic sciences. Mar. Ecol. Prog. Ser., 446, 285-302, 2012.

Leavitt, W. D., Halevy, I., Bradley, A. S., and Johnston, D. T.: Influence of sulfate reduction rates on the Phanerozoic sulfur isotope record. P. Natl. Acad. Sci. USA, 110, 11244-11249, 2013.

Lehto, N., Glud, R.N., á Norði, G., Zhang, H., and Davison, W.: Anoxic microniches in marine sediments induced by aggregate settlement: biogeochemical dynamics and implications. Biogeochemistry, 119, 307-327, 2014.

Lehtoranta, J., Ekholm, P., and Pitkänen, H.: Coastal eutrophication thresholds: a matter of sediment microbial processes. AMBIO, 38, 303-308, 2009.

Lenstra, W. K., Hermans, M., Séguret, M. J., Witbaard, R., Behrends, T., Dijkstra, N., van Helmond, N. A., Kraal, P., Laan, P., Rijkenberg, M. J., and Severmann, S.: The shelf-to-basin iron shuttle in the Black Sea revisited. Chem. Geol., 511, 314-341, 2019.

Levin, L. A., Rathburn, A. E., Gutiérrez, D., Muñoz, P., and Shankle, A.: Bioturbation by symbiont-bearing annelids in near-anoxic sediments: implications for biofacies models and paleo-oxygen assessments. Palaeogeogr. Palaeoclimatol. Palaeoecol., 199, 129-140, 2003.

Lewy, Z., and Samtleben, C.: Functional morphology and palaeontological significance of the conchiolin layers in corbulid pelecypods. Lethaia, 12, 341-351, 1979.

Liu, A. G., McMahon, S., Matthews, J. J., Still, J. W., and Brasier, A. T.: Petrological evidence supports the death mask model for the preservation of Ediacaran soft-bodied organisms in South Australia. Geology, 47, 215-218, 2019.

Lohrer, A. M., Thrush, S. F., and Gibbs, M. M.: Bioturbators enhance ecosystem function through complex biogeochemical interactions. Nature, 431, 1092-1095, 2004.

870   Loope, D. B., and Watkins, D. K.: Pennsylvanian fossils replaced by red chert; early oxidation of pyritic precursors. J. Sediment. Res., 59, 375-386, 1989.

Machain-Castillo, M. L., Ruiz-Fernández, A. C., Gracia, A., Sanchez-Cabeza, J. A., Rodríguez-Ramírez, A., Alexander-Valdés, H. M., Pérez-Bernal, L. H., Nava-Fernández, X. A., Gómez-Lizárraga, L. E., Almaraz-Ruiz, L., and Schwing, P. T.: Natural and anthropogenic oil impacts on benthic foraminifera in the southern Gulf of Mexico. Mar. Environ. Res., 149, 111-
875   125, 2019.

Maire, O., Lecroart, P., Meysman, F., Rosenberg, R., Duchêne, J. C., and Grémare, A.: Quantification of sediment reworking rates in bioturbation research: a review. Aquat. Biol., 2, 219-238, 2008.

Marchetti, R., Provini, A., and Crosa, G.: Nutrient load carried by the River Po into the Adriatic Sea, 1968–1987. Mar. Pollut. Bull, 20, 168-172, 1989.

880   Mautner, A. K., Gallmetzer, I., Haselmair, A., Schnedl, S. M., Tomašových, A., and Zuschin, M.: Holocene ecosystem shifts and human-induced loss of Arca and Ostrea shell beds in the north-eastern Adriatic Sea. Mar. Pollut. Bull., 126, 19-30, 2018.

Meadows, A., Meadows, P. S., West, F. J. and Murray, J. M.: Bioturbation, geochemistry and geotechnics of sediments affected by the oxygen minimum zone on the Oman continental slope and abyssal plain, Arabian Sea. Deep-Sea Res. Pt. II, 47, 259-280, 2000.

885   Meile, C., and Van Cappellen, P.: Particle age distributions and O2 exposure times: timescales in bioturbated sediments. Global Biochem. Cy., 19, GB3013, 2005.

Mermillod-Blondin, F., and Rosenberg, R.: Ecosystem engineering: the impact of bioturbation on biogeochemical processes in marine and freshwater benthic habitats. Aquat. Sci., 68, 434-442, 2006.

Mermillod-Blondin, F.: The functional significance of bioturbation and biodeposition on biogeochemical processes at the
890   water–sediment interface in freshwater and marine ecosystems. J. N. Am. Benthol. Soc., 30, 770-778, 2011.

Meysman, F. J., Boudreau, B. P., and Middelburg, J. J.: Relations between local, nonlocal, discrete and continuous models of bioturbation. J. Mar. Res., 61, 391-410, 2003.

Middelburg, J. J., and Levin, L. A.: Coastal hypoxia and sediment biogeochemistry. Biogeosciences 6, 1273-1293, 2009.

Meysman, F. J., Galaktionov, O. S., Gribsholt, B., and Middelburg, J. J.: Bioirrigation in permeable sediments: Advective
895   pore-water transport induced by burrow ventilation. Limnol. Oceanogr., 51, 142-156, 2006.

Moodley, L., Heip, C. H., and Middelburg, J. J.: Benthic activity in sediments of the northwestern Adriatic Sea: sediment oxygen consumption, macro-and meiofauna dynamics. J. Sea Res., 40, 263-280, 1998.

Moodley, L., Chen, G., Heip, C., and Vincx, M.: Vertical distribution of meiofauna in sediments from contrasting sites in the Adriatic Sea: clues to the role of abiotic versus biotic control. Ophelia, 53, 203-212, 2000.

900   Nebelsick, J. H., Schmid, B., and Stachowitsch, M.: The encrustation of fossil and recent sea-urchin tests: ecological and
        taphonomic significance. Lethaia, 30, 271-284, 1997.

        Neumann, T., Rausch, N., Leipe, T., Dellwig, O., Berner, Z., and Böttcher, M. E.: Intense pyrite formation under low-sulfate
        conditions in the Achterwasser lagoon, SW Baltic Sea. Geochim. Cosmochim. Ac., 69, 3619-3630, 2005.

        Nilsson, H. C., and Rosenberg, R.: Succession in marine benthic habitats and fauna in response to oxygen deficiency:
905   analysed by sediment profile-imaging and by grab samples. Mar. Ecol. Prog. Ser., 197, 139-149, 2000.

        Novek, J. M., Dornbos, S. Q., and McHenry, L. J.: Palaeoredox geochemistry and bioturbation levels of the exceptionally
        preserved early Cambrian Indian Springs biota, Nevada, USA. Lethaia, 49, 604-616, 2016.

        N'Siala, G. M., Grandi, V., Iotti, M., Montanari, G., Prevedelli, D., and Simonini, R.: Responses of a northern Adriatic
        Ampelisca–Corbula community to seasonality and short-term hydrological changes in the Po river. Mar. Environ. Res., 66,
910   466-476, 2008.

        Occhipinti-Ambrogi, A., Savini, D., and Forni, G.: Macrobenthos community structural changes off Cesenatico coast (Emilia
        Romagna, Northern Adriatic), a six-year monitoring programme. Sci. Total. Environ., 353, 317-328, 2005.

        Ogrinc, N., and Faganeli, J.: Stable carbon isotopes in pore waters of coastal marine sediments (the Gulf of Trieste, N
        Adriatic). Acta Chim. Slov., 50, 645-662, 2003.

915   Pakhomova, S. V., Hall, P. O., Kononets, M. Y., Rozanov, A. G., Tengberg, A., and Vershinin, A. V.: Fluxes of iron and
        manganese across the sediment–water interface under various redox conditions. Mar. Chem., 107, 319-331, 2007.

        Palinkas, C. M., and Nittrouer, C. A.: Modern sediment accumulation on the Po shelf, Adriatic Sea. Cont. Shelf Res., 27,
        489-505, 2007.

        Paul, C.R.C., Allison, P.A. and Brett, C.E.: The occurrence and preservation of ammonites in the Blue Lias Formation
920   (lower Jurassic) of Devon and Dorset, England and their palaeoecological, sedimentological and diagenetic
        significance. Palaeogeogr. Palaeoclimatol. Palaeoecol., 270, 258-272, 2008.

        Penna, N., Rinaldi, A., Montanari, G., Di Paolo, A., and Penna, A.: Mucilaginous masses in the Adriatic Sea in the summer
        of 1989. Water Res., 27, 1767-1771, 1993.

        Pirlet, H., Wehrmann, L. M., Brunner, B., Frank, N., Dewanckele, J. A. N., Van Rooij, D., Foubert, A., Swennen, R.,
925   Naudts, L., Boone, M., and Cnudde, V.: Diagenetic formation of gypsum and dolomite in a cold-water coral mound in the
        Porcupine Seabight, off Ireland. Sedimentology, 57, 786-805, 2010.

        Powell, E. N., and Stanton R. J., Jr.: Estimating biomass and energy flow of molluscs in
        palaeocommunities. Palaeontology, 28, 1-34, 1985.

        Powell, E. N., Hu, X., Cai, W. J., Ashton-Alcox, K. A., Parsons-Hubbard, K. M. and Walker, S. E.: Geochemical controls on
930   carbonate shell taphonomy in Northern Gulf of Mexico continental shelf and slope sediments. Palaios, 27, 571-584, 2012.

        Precali, R., Giani, M., Marini, M., Grilli, F., Ferrari, C. R., Pečar, O. and Paschini, E.: Mucilaginous aggregates in the
        northern Adriatic in the period 1999–2002: typology and distribution. Sci. Total. Environ., 353, 10-23, 2005.

Pruss, S., Fraiser, M., and Bottjer, D. J.: Proliferation of Early Triassic wrinkle structures: implications for environmental stress following the end-Permian mass extinction. Geology, 32, 461-464, 2004.

935   Raiswell, R., Whaler, K., Dean, S., Coleman, M. L., and Briggs, D. E. G.: A simple three-dimensional model of diffusion-with-precipitation applied to localised pyrite formation in framboids, fossils and detrital iron minerals. Mar. Geol., 113, 89-100, 1993.

Raiswell, R., and Canfield, D. E.: Rates of reaction between silicate iron and dissolved sulfide in Peru Margin sediments. Geochim. Cosmochim. Ac., 60, 2777-2787, 1996.

940   Renz, J. R., Powilleit, M., Gogina, M., Zettler, M. L., Morys, C., and Forster, S.: Community bioirrigation potential (BIPc), an index to quantify the potential for solute exchange at the sediment-water interface. Mar. Environ. Res., 141, 214-224, 2018.

Reolid, M.: Pyritized radiolarians and siliceous sponges from oxygen-restricted deposits (Lower Toarcian, Jurassic). Facies, 60, 789-799, 2014.

945   Rhoads, D. C., and Germano, J. D.: Interpreting long-term changes in benthic community structure: a new protocol. Hydrobiologia, 142, 291 – 308, 1986.

Rosenberg, R., Nilsson, H. C., and Diaz, R. J.: Response of benthic fauna and changing sediment redox profiles over a hypoxic gradient. Estuar. Coast. Shelf S., 53, 343-350, 2001.

Saleh, F., Pittet, B., Perrillat, J. P., and Lefebvre, B.: Orbital control on exceptional fossil preservation. Geology, 47, 103-106, 2019.

950

Saleh, F., Pittet, B., Sansjofre, P., Guériau, P., Lalonde, S., Perrillat, J. P., Vidal, M., Lucas, V., El Hariri, K., Kouraiss, K., and Lefebvre, B.: Taphonomic pathway of exceptionally preserved fossils in the Lower Ordovician of Morocco. Geobios, 2020.

Sandnes, J., Forbes, T., Hansen, R., Sandnes, B., and Rygg, B.: Bioturbation and irrigation in natural sediments, described by animal-community parameters. Mar. Ecol. Prog. Ser., 197, 169-179, 2000.

955

Sangiorgi, F., and Donders, T. H.: Reconstructing 150 years of eutrophication in the north-western Adriatic Sea (Italy) using dinoflagellate cysts, pollen and spores. Estuar. Coast. Shelf S., 60, 69-79, 2004.

Savrda, C. E., and Ozalas, K.: Preservation of mixed-layer ichnofabrics in oxygenation-event beds. Palaios, 8, 609-612, 1993.

960   Schaffner, L. C., Jonsson, P., Diaz, R. J., Rosenberg, R., and Gapcynski, P.: Benthic communities and bioturbation history of estuarine and coastal systems: effects of hypoxia and anoxia. Marine Coastal Eutrophication (pp. 1001-1016). Elsevier, 1992.

Schieber, J., and Baird, G.: On the origin and significance of pyrite spheres in Devonian black shales of North America. J. Sediment. Res., 71, 155-166, 2001.

965   Schieber, J.: Styles of agglutination in benthic foraminifera from modern Santa Barbara Basin sediments and the implications of finding fossil analogs in Devonian and Mississippian black shales. In Anoxia (pp. 573-589). Springer, Dordrecht, 2012.

Schiffbauer, J. D., Xiao, S., Cai, Y., Wallace, A. F., Hua, H., Hunter, J., Xu, H., Peng, Y., and Kaufman, A. J.: A unifying model for Neoproterozoic–Palaeozoic exceptional fossil preservation through pyritization and carbonaceous 970   compression. Nat. Commun., 5, 1-12, 2014.

Schinner, G. O. F.: Burrowing behavior, substratum preference, and distribution of Schizaster canaliferus (Echinoidea: Spatangoida) in the northern Adriatic Sea. Mar. Ecol., 14, 129-145, 1993.

Schinner, F. Stachowitsch, M, and Hilgers, H.: Loss of benthic communities: warning signal for coastal ecosystem management. Aq. Cons.: Mar. Freshw. Ecosyst. 6, 343-352, 1997.

975   Schnedl, S. M., Haselmair, A., Gallmetzer, I., Mautner, A. K., Tomašových, A., and Zuschin, M.: Molluscan benthic communities at Brijuni Islands (northern Adriatic Sea) shaped by Holocene sea-level rise and recent human eutrophication and pollution. Holocene, 28, 1801-1817, 2018.

Slagter, S., Tarhan, L. G., Hao, W., Planavsky, N. J., and Konhauser, K. O.: Experimental evidence supports early silica cementation of the Ediacara Biota. Geology, 49, 51-55, 2021.

980   Smith, C. R., Levin, L. A., Hoover, D. J., McMurtry, G., and Gage, J. D.: Variations in bioturbation across the oxygen minimum zone in the northwest Arabian Sea. Deep-Sea Res. Pt. II, 47, 227-257, 2000.

Solan, M., and Kennedy, R.: Observation and quantification of in situ animal-sediment relations using time-lapse sediment profile imagery (t-SPI). Mar. Ecol. Prog. Ser., 228, 179-191, 2002.

Solan, M., Cardinale, B. J., Downing, A. L., Engelhardt, K. A., Ruesink, J. L., and Srivastava, D. S.: Extinction and 985   ecosystem function in the marine benthos. Science, 306, 1177-1180, 2004.

Solan, M., Ward, E. R., White, E. L., Hibberd, E. E., Cassidy, C., Schuster, J. M., Hale, R., and Godbold, J. A.: Worldwide measurements of bioturbation intensity, ventilation rate, and the mixing depth of marine sediments. Sci. Data, 6, 1-6, 2019.

Solis-Weiss, V., Aleffi, F., Bettoso, N., Rossi, R., and Orel, G.: The benthic macrofauna at the outfalls of the underwater sewage discharges in the Gulf of Trieste (northern Adriatic Sea). Ann. Ser. Hist. Natur., 17, 1-16, 2007.

990   Spagnoli, F., Dinelli, E., Giordano, P., Marcaccio, M., Zaffagnini, F., and Frascari, F.: Sedimentological, biogeochemical and mineralogical facies of Northern and Central Western Adriatic Sea. J. Marine Syst., 139, 183-203, 2014.

Stachowitsch, M.: Mass mortality in the Gulf of Trieste: the course of community destruction. Mar. Ecol., 5, 243-264, 1984.

Stachowitsch, M.: Anoxia in the Northern Adriatic Sea: rapid death, slow recovery. Geol. Soc. Spec. Publ., 58, 119-129, 1991.

995   Steckbauer, A., Duarte, C. M., Carstensen, J., Vaquer-Sunyer, R., and Conley, D. J.: Ecosystem impacts of hypoxia: thresholds of hypoxia and pathways to recovery. Environ. Res. Lett., 6, 025003, 2011.

Stefanon, A. T., and Boldrin, A.: The oxygen crisis of the northern Adriatic Sea waters in late fall 1977 and its effects on benthic communities. In Proceedings of 6th International Science Symposium World Underwater Federation (CMAS),

edited by: Blanchard, J., Mair, J., and Morrison, I., National Environmental Research Council, Edinburgh (pp. 167-175),
1000   1982.

Stockdale, A., Davison, W., and Zhang, H.: Formation of iron sulfide at faecal pellets and other microniches within suboxic
surface sediment. Geochim. Cosmochim. Ac., 74, 2665-2676, 2010.

Strang, K. M., Armstrong, H. A., Harper, D. A., and Trabucho-Alexandre, J. P.: The Sirius Passet Lagerstätte: silica death
masking opens the window on the earliest matground community of the Cambrian explosion. Lethaia, 49, 631-643, 2016.

1005   Tarhan, L. G., Droser, M. L., Planavsky, N. J., and Johnston, D. T.: Protracted development of bioturbation through the early
Palaeozoic Era. Nat. Geosci., 8, 865-869, 2015.

Tarhan, L. G., Hood, A. V., Droser, M. L., Gehling, J. G., and Briggs, D. E.: Exceptional preservation of soft-bodied
Ediacara Biota promoted by silica-rich oceans. Geology, 44, 951-954, 2016.

Taylor, A., Goldring, R., and Gowland, S.: Analysis and application of ichnofabrics. Earth-Sci. Rev., 60, 227-259, 2003.

1010   Teal, L. R., Bulling, M. T., Parker, E. R., and Solan, M.: Global patterns of bioturbation intensity and mixed depth of marine
soft sediments. Aquat. Biol., 2, 207-218, 2008.

Teal, L. R., Parker, E. R., and Solan, M.: Sediment mixed layer as a proxy for benthic ecosystem process and function. Mar.
Ecol. Prog. Ser., 414, 27-40, 2010.

Tesi, T., Langone, L., Goñi, M. A., Wheatcroft, R. A., Miserocchi, S., and Bertotti, L.: Early diagenesis of recently deposited
1015   organic matter: A 9-yr time-series study of a flood deposit. Geochim. Cosmochim. Ac., 83, 19-36, 2012.

Thayer, C. W.: Sediment-mediated biological disturbance and the evolution of marine benthos. In Biotic interactions in
recent and fossil benthic communities (pp. 479-625). Springer, Boston, MA, 1983.

Thomsen, E., and Vorren, T. O.: Pyritization of tubes and burrows from Late Pleistocene continental shelf sediments off
North Norway. Sedimentology, 31, 481-492, 1984.

1020   Tomašových, A., Kidwell, S. M., Barber, R. F., and Kaufman, D. S.: Long-term accumulation of carbonate shells reflects a
100-fold drop in loss rate. Geology, 42, 819-822, 2014.

Tomašových, A., Gallmetzer, I., Haselmair, A., Kaufman, D. S., Vidović, J., and Zuschin, M.: Stratigraphic unmixing
reveals repeated hypoxia events over the past 500 yr in the northern Adriatic Sea. Geology, 45, 363-366, 2017.

Tomašových, A., Gallmetzer, I., Haselmair, A., Kaufman, D.S., Kralj, M., Cassin, D., Zonta, R. and Zuschin, M., 2018.
1025   Tracing the effects of eutrophication on molluscan communities in sediment cores: outbreaks of an opportunistic species
coincide with reduced bioturbation and high frequency of hypoxia in the Adriatic Sea. Paleobiology, 44, 575-602.

Tomašových, A., Gallmetzer, I., Haselmair, A., Kaufman, D. S., Mavrič, B., and Zuschin, M.: A decline in molluscan
carbonate production driven by the loss of vegetated habitats encoded in the Holocene sedimentary record of the Gulf of
Trieste. Sedimentology, 66, 781-807, 2019a.

1030   Tomašových, A., Kidwell, S. M., Alexander, C. R., and Kaufman, D. S.: Millennial-scale age offsets within fossil
assemblages: Result of bioturbation below the taphonomic active zone and out-of-phase production. Paleoceanogr.
Paleocl., 34, 954-977, 2019b.

Tomašových, A., Albano, P. G., Fuksi, T., Gallmetzer, I., Haselmair, A., Kowalewski, M., Nawrot, R., Nerlović, V., Scarponi, D., and Zuschin, M.: Ecological regime shift preserved in the Anthropocene stratigraphic record. P. Roy. Soc. B-Biol Sci, 287, 20200695, 2020.

Underwood, C. J., and Bottrell, S. H.: Diagenetic controls on multiphase pyritization of graptolites. Geol. Mag., 131, 315-327, 1994.

Valente, R. M., and Cuomo, C.: Did multiple sediment-associated stressors contribute to the 1999 lobster mass mortality event in Western Long Island Sound, USA? Estuaries, 28, 529-540, 2005.

van de Velde, S., and Meysman, F. J.: The influence of bioturbation on iron and sulphur cycling in marine sediments: a model analysis. Aquat. Geochem., 22, 469-504, 2016.

Vatova A.: La fauna bentonica dell'alto e medio Adriatico. Nova Thalassia 1, 1-110, 1949.

Virtasalo, J. J., Löwemark, L., Papunen, H., Kotilainen, A. T., and Whitehouse, M. J.: Pyritic and baritic burrows and microbial filaments in postglacial lacustrine clays in the northern Baltic Sea. J. Geol. Soc. London, 167, 1185-1198, 2010.

Virtasalo, J. J., Whitehouse, M. J., and Kotilainen, A. T.: Iron isotope heterogeneity in pyrite fillings of Holocene worm burrows. Geology, 41, 39-42, 2013.

Vopel, K., Thistle, D., and Rosenberg, R.: Effect of the brittle star Amphiura filiformis (Amphiuridae, Echinodermata) on oxygen flux into the sediment. Limnol. Oceanogr., 48, 2034-2045, 2003.

Walker, S. E., and Goldstein, S. T.: Taphonomic tiering: experimental field taphonomy of molluscs and foraminifera above and below the sediment–water interface. Palaeogeogr. Palaeoclimatol. Palaeoecol., 149, 227-244, 1999.

Westall, F.: The nature of fossil bacteria: a guide to the search for extraterrestrial life. J. Geophys. Res.-Planets, 104, 16437-16451, 1999.

Wignall, P. B., Newton, R., and Brookfield, M. E.: Pyrite framboid evidence for oxygen-poor deposition during the Permian–Triassic crisis in Kashmir. Palaeogeogr. Palaeoclimatol. Palaeoecol., 216, 183-188, 2005.

Wijsman, J. W. M., Herman, P. M. J., Middelburg, J. J., and Soetaert, K.: A model for early diagenetic processes in sediments of the continental shelf of the Black Sea. Estuar. Coast. Shelf S., 54, 403-421, 2002.

Wilson, M. A., and Taylor, P. D.: Exceptional pyritized cyanobacterial mats encrusting brachiopod shells from the Upper Ordovician (Katian) of the Cincinnati, Ohio, region. Palaios, 32, 673-677, 2017.

Wheatcroft, R. A.: Preservation potential of sedimentary event layers. Geology, 18, 843-845, 1990.

Zhu, M., Babcock, L. E., and Steiner, M.: Fossilization modes in the Chengjiang Lagerstätte (Cambrian of China): testing the roles of organic preservation and diagenetic alteration in exceptional preservation. Palaeogeogr. Palaeoclimatol. Palaeoecol.,, 31-46, 2005.

Zillén, L., Conley, D. J., Andrén, T., Andrén, E., and Björck, S.: Past occurrences of hypoxia in the Baltic Sea and the role of climate variability, environmental change and human impact. Earth-Sci. Rev., 91, 77-92, 2008.

1065   Zuschin, M., Stachowitsch, M., Pervesler, P., and Kollmann, H.: Structural features and taphonomic pathways of a high-biomass epifauna in the northern Gulf of Trieste, Adriatic Sea. Lethaia, 32, 299-316, 1999.

Zuschin, M., and Stachowitsch, M.: Epifauna-dominated benthic shelf assemblages: lessons from the modern Adriatic Sea. Palaios, 24, 211-221, 2009.

1070
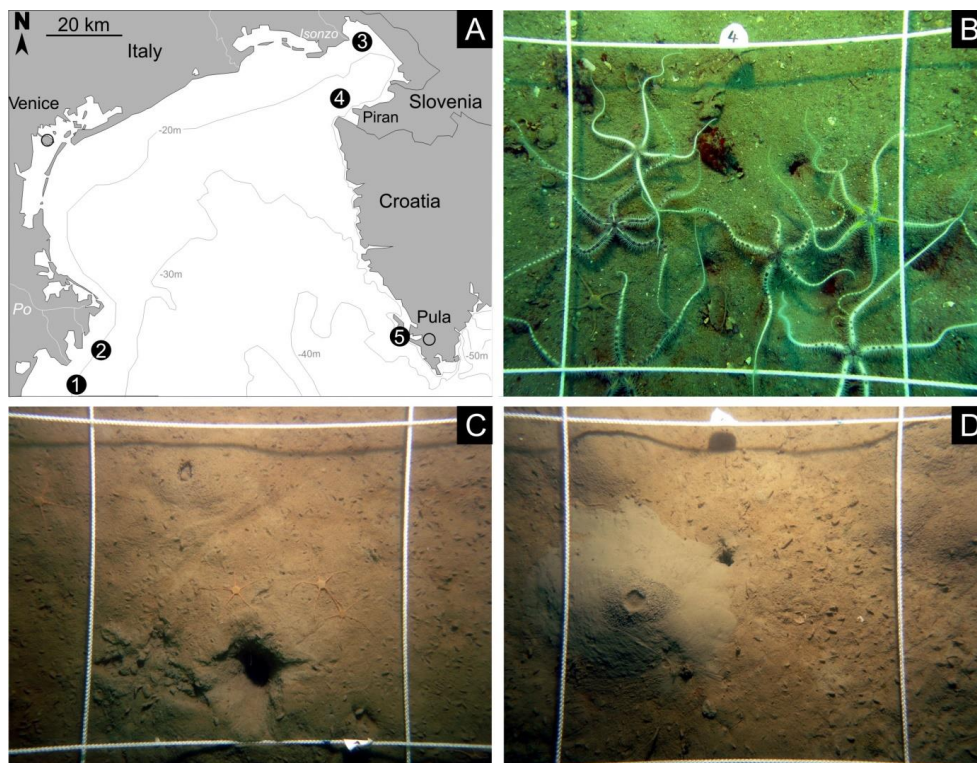
Figure 1 – A. Geographic map with the locations of five sites analyzed in this study: 1 – Po 4 (with two replicate cores M20 and M21), 2 - Po 3 (with two replicate cores M13 and M14), 3 – Bay of Panzano in the northern Gulf of Trieste (with two sediment cores M28 and M29), 4 – Piran (M53 core) and 5 – Brijuni (M44). B-D. Sea floor photographs taken in 2014 at
1075   Piran (B, with abundant *Ophiotrix*), Po 4 (C, with abundant *Ophiura albida*) and Po 3 (D) documenting abundant burrow and mound structures and uneven topography. The size of the square is 25 cm^2. The thickness of the mixed layer at Po is ~20 cm on the basis of both ^{14}C and ^{210}Pb and also at Brijuni, and ~ 8 cm at Piran, underlain by a shell bed.
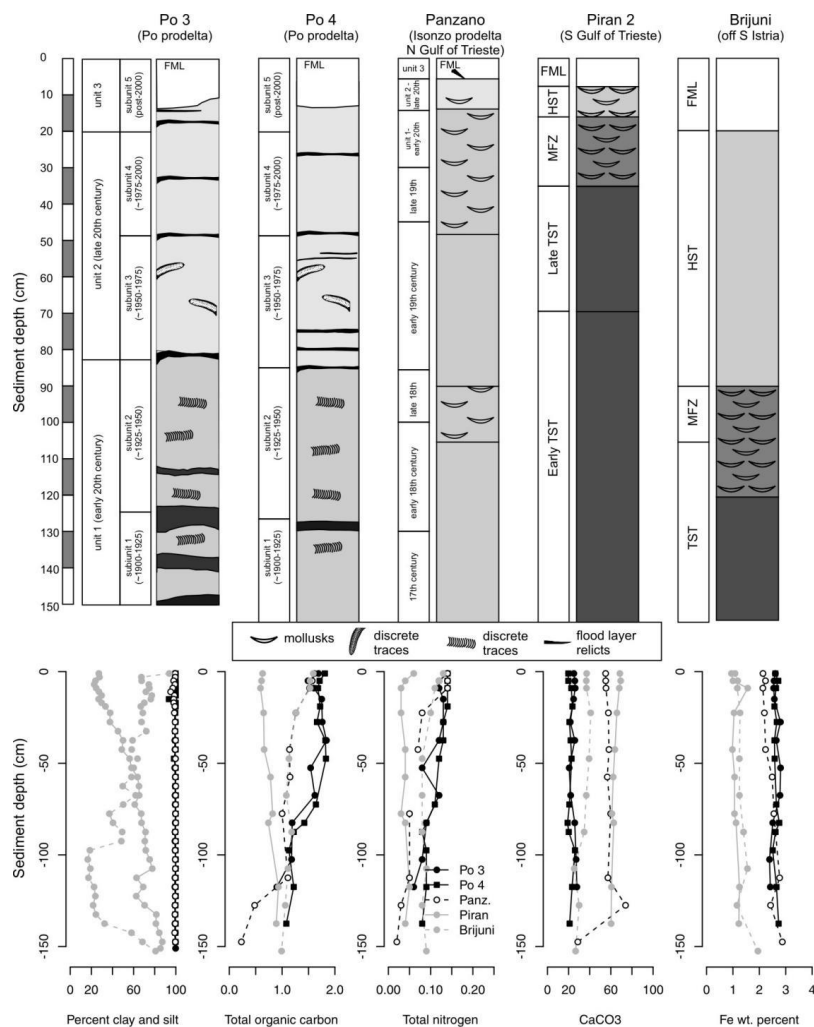
Figure 2 – Top row: Lithologic sections through sediment cores at five locations, with the highest sedimentation rate (1-2 cm/y) at Po stations, intermediate net sedimentation rate (0.2-0.4 cm/y) in the Bay of Panzano, and very slow sedimentation rate at Piran and Brijuni (~0.01 cm/y), with chronostratigraphic subdivisions. TST – transgressive systems tract, MFZ – maximum flooding zone, HST – highstand systems tract, FML – mixed layer. Bottom row: Stratigraphic trends in grain size, total organic carbon and nitrogen (TOC and TN), CaCO₃ (based on total inorganic carbon), and the weight percent of iron also discriminate between sites with higher sedimentation (Po and Panzano) and sites with slower sedimentation (Piran and Brijuni).
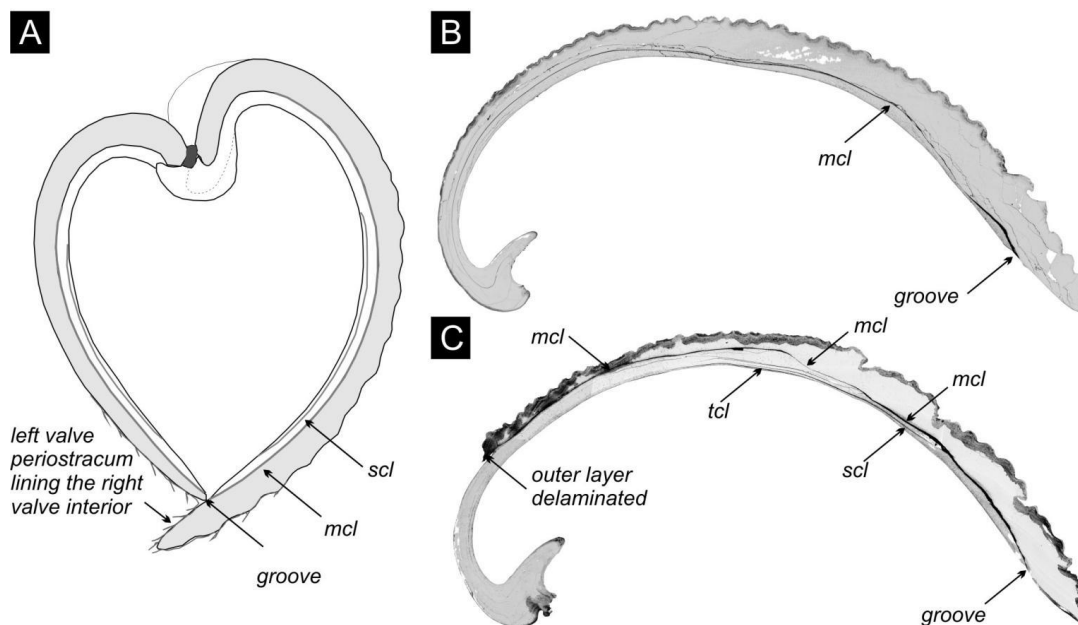
1090

Figure 3 – A. The cross-section of the articulated shell of *V. gibba*, modified according to Lewy and Samtleben (1979), shows that the internal conchiolin layer (mcl) separates both valves into an inner later and an outer layer, and the inner layer can contain another secondary conchiolin layer (scl). The left valve fits into a groove with the conchiolin layer on the interior of the right valve. Periostracum on the left valve extends beyond its length and covers the interior of the right valve. B. The section through the right valve with a cavity (in black) initially filled by the single (main) conchiolin layer. Po 3 (core M14) at 40-45 cm. C. The section through the right valve with 10-100 µm-thick cavities (mcl – main conchiolin layer, scl - secondary conchiolin layer, tcl - tertiary conchiolin layer) left by several conchiolin layers (some cavities are still filled by carbonate nodules or by pyrite). Po 3 (core M13) at 65-70 cm.

1100
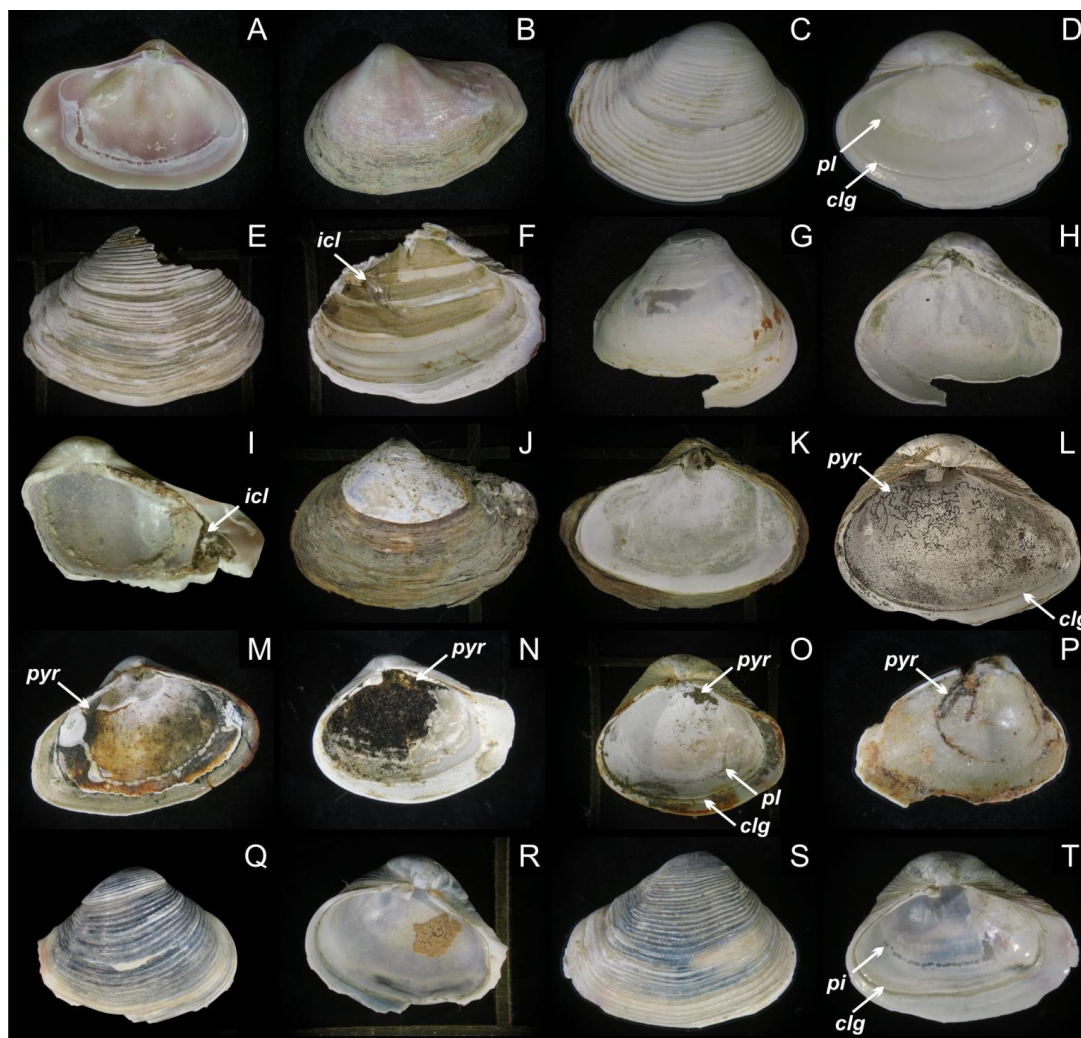
Figure 4 - *Varicorbula gibba* from Po and Panzano stations (characterized by high sedimentation rates), showing the variability in external and internal preservation, with well-preserved valves with (A-B) or without periostracum (C-D). The interiors of some specimens are lined by pyritic framboids that form isolated and dispersed framboids (A), strings (B), and patchy or continuous coatings on the conchiolin layer (C-F). These specimens tend to be associated with brownish grains and streaks and with surface internal dissolution. Some specimen have blueish color (U-X). A-B. Left valve, M28-65-70 cm-29,C-D. Right valve, M21-90-95 cm-1. E-F. Outer layer of the right valve, M13-65-70 cm-25. G-H. Inner layer of the right valve, M13-20-25 cm-8, I. Internal conchiolin layer exposed in a fragment, M20-120-125 cm. J-K. Left valve with periostracum and finely dispersed pyrite framboids on interior, M21-2-4 cm-2, L. Interior of the right valve with strings of pyrite framboids, M21-90-95 cm, M. Interior of the left valve lined by pyrite framboids, M28-110-115 cm-22, N. Interior of the right valve almost continuously lined by pyrite framboids, M28-110-115 cm-14, O. Interior of the right valve lined by patches of pyrite framboids, M21-30-35 cm-29, P. Interior of the left valve with strings of oxidixed pyrite framboids, M28-125-130 cm-21, Q-R. Blue-stained right valve, M28-85-90 cm-1. S-T. Blue-stained right valve, M21-105-110 cm-4. Note: clg – conchiolin groove, pl – pallial line, pyr – framboidal pyrite, icl - internal conchiolin layer.
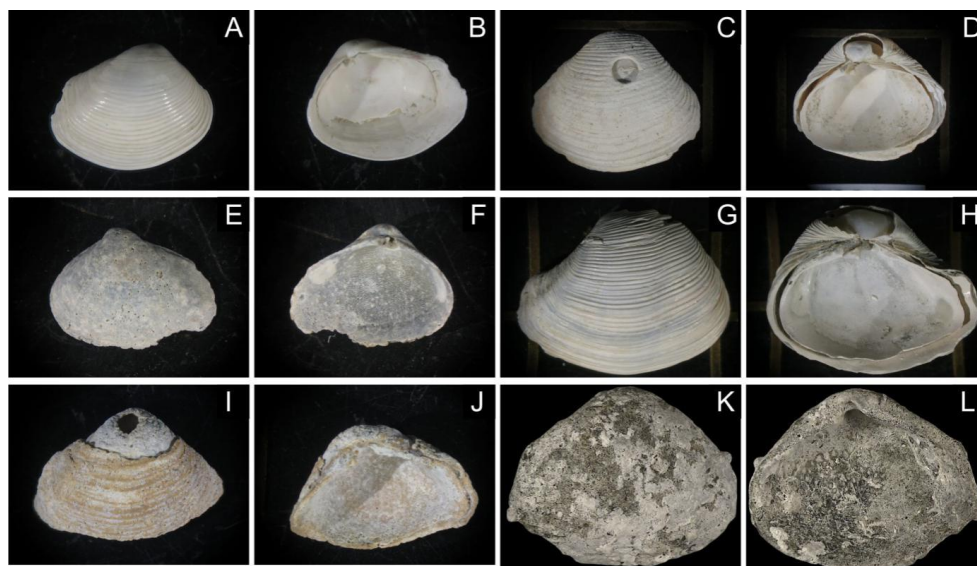
1115

Figure 5 – *Varicorbula gibba* from a Piran and Brijuni stations (sites with slow sedimentation) with worn, bored, encrusted and stained valves. A-B. M53-0-2 cm-7, C-D. M53-0-2 cm-6, E-F. M53-0-2 cm-4, G-H. M53-100-105 cm-1, I-J. M53-0-2 cm-2, K-L. M44-140-145 cm.
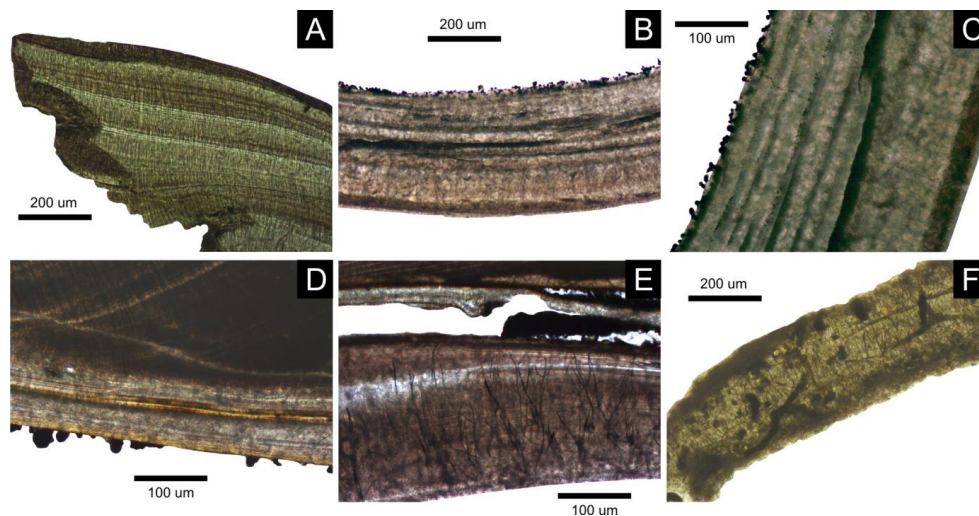
Figure 6 – Thin-section photographs showing pyrite framboids on the inner surface of *V. gibba* and preservation of more altered valves. A – A pristine right valve not lined by pyrite framboids, M13-65-79 cm-29. B-C - Internal surface of well-preserved right valve lined by pyrite framboids, M21-90-95 cm. D - Internal surface of well-preserved right valve lined by pyrite framboids, M14-40-45 cm. E – Internal conchiolin layer with a dark-stained mixture of carbonate nodules and pyrite rimmed by Fe oxides, M20-120-125 cm. F – Strongly bored valve filled micrite and stained by nanopyritic inclusions, M44-140-145 cm.
Figure 7 - Backscattered electron images showing pyrite framboids on *V. gibba* valve interiors and in the main conchiolin
layer in well-preserved valves and pyrite framboids and nanopyrite in microborings or microfractures in highly altered
valves. A-D – Pyrite framboids attached to the interior surface, Po 3 (M14)-40-45 cm. E-F – Pyrite framboids attached to the
interior surface, Po 4 (M21)-90-95 cm. G-I – Pyrite framboids on the interior and framboids (located between aragonite
nodules) rimmed by Fe oxides in the main conchiolin layer, Po 4 (M20)-120-125 cm. J-K – a well-preserved specimen
without microborings but with blueish staining contain nanopyritic inclusions (aggregation of micro-sized microcystals),
Piran (M53)-100-105 cm-1. L – a dark-stained specimen with intense microborings, encrusters and cementation of pores and
borings filled by framboids (sp - secondary pyrite lining), by nanopyritic inclusions (np), and by high-Mg calcite (darker
infills), Brijuni (M44)-140-145 cm-2 –Scale bars: A, E, H – 100 μm, B-D, F, G, I-L - 10 μm.
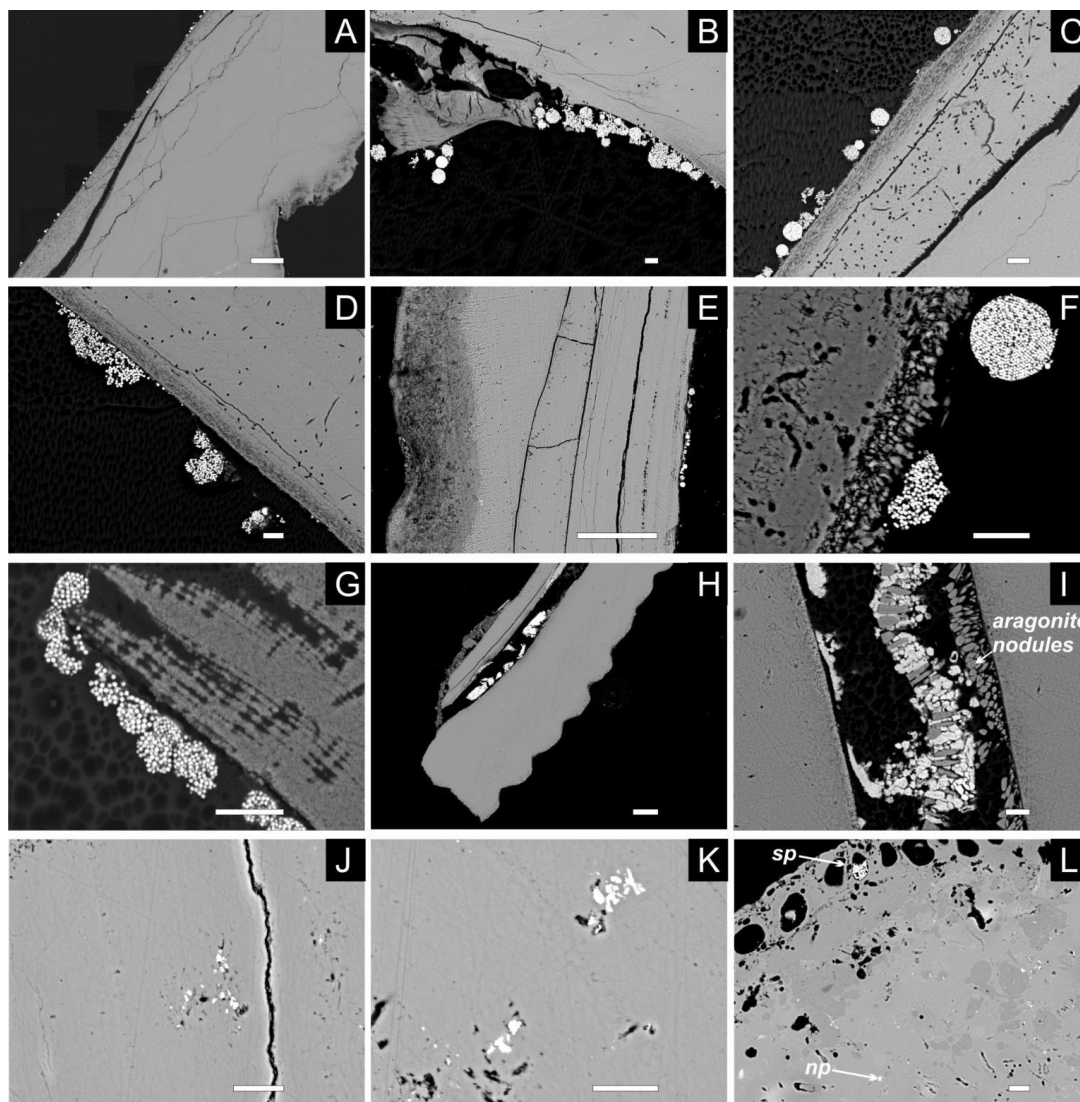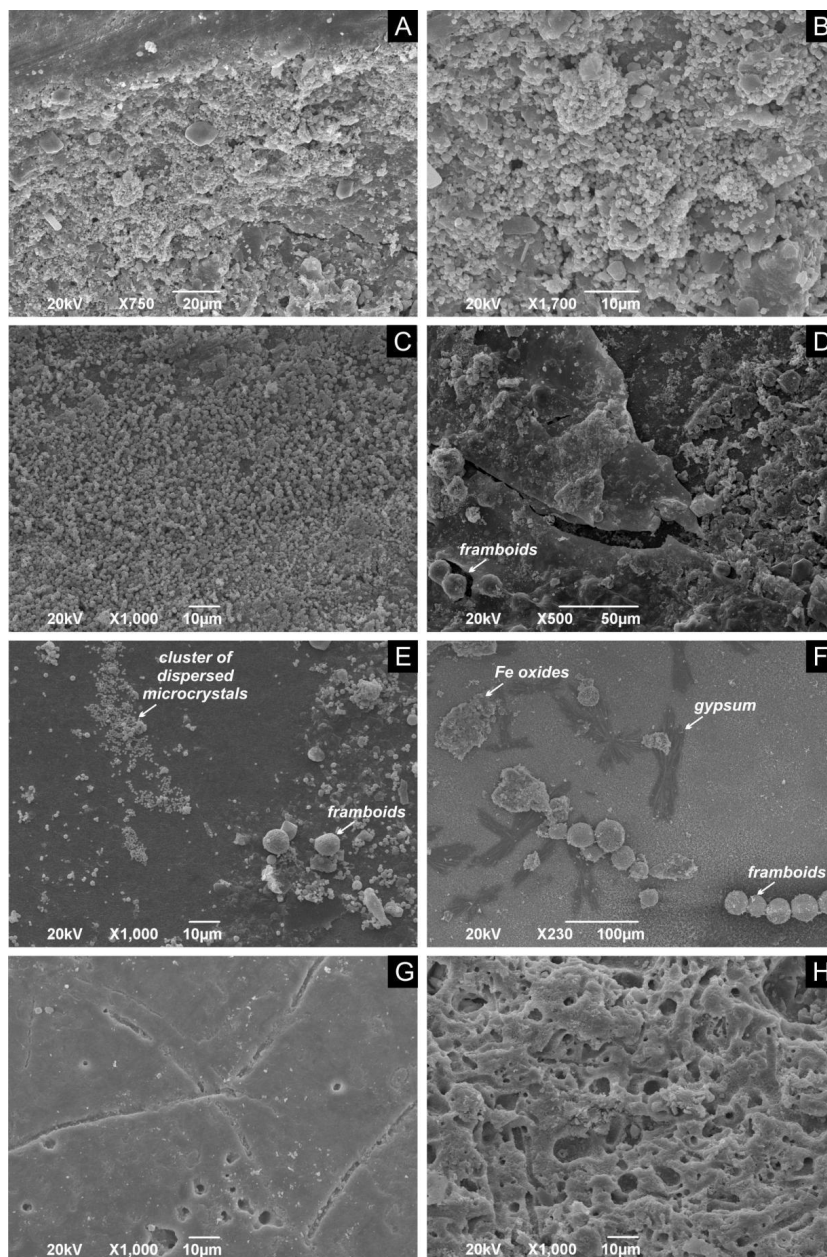
Figure 8 – Internal surfaces of *V. gibba* with isolated and clustered framboids on well-preserved valves from Po and with
intense borings on valves from Brijuni. A-B – Dispersed pyrite microcrystals and isolated framboids clustered around the
groove at which the internal conchiolin crops out. C – Dispersed pyrite microcrystals close to the groove. D – Sheets of
organics underlain by framboids on the interior of the right valve close to the ventral margin. E – Clusters of dispersed
microcrystals and isolated framboids on the well-preserved ventral valve margin. F – Strings of pyrite framboids, irregular
flakes of Fe oxides, and small gypsum crystals. G, H – moderate (G) and strong bioerosion (H). A-B - Po4-30-35 cm-28, D-
F - Po4-30-35 cm-28, G - Brijuni-M44-70-75 cm-3, H - Brijuni-M44-70-75 cm-1.
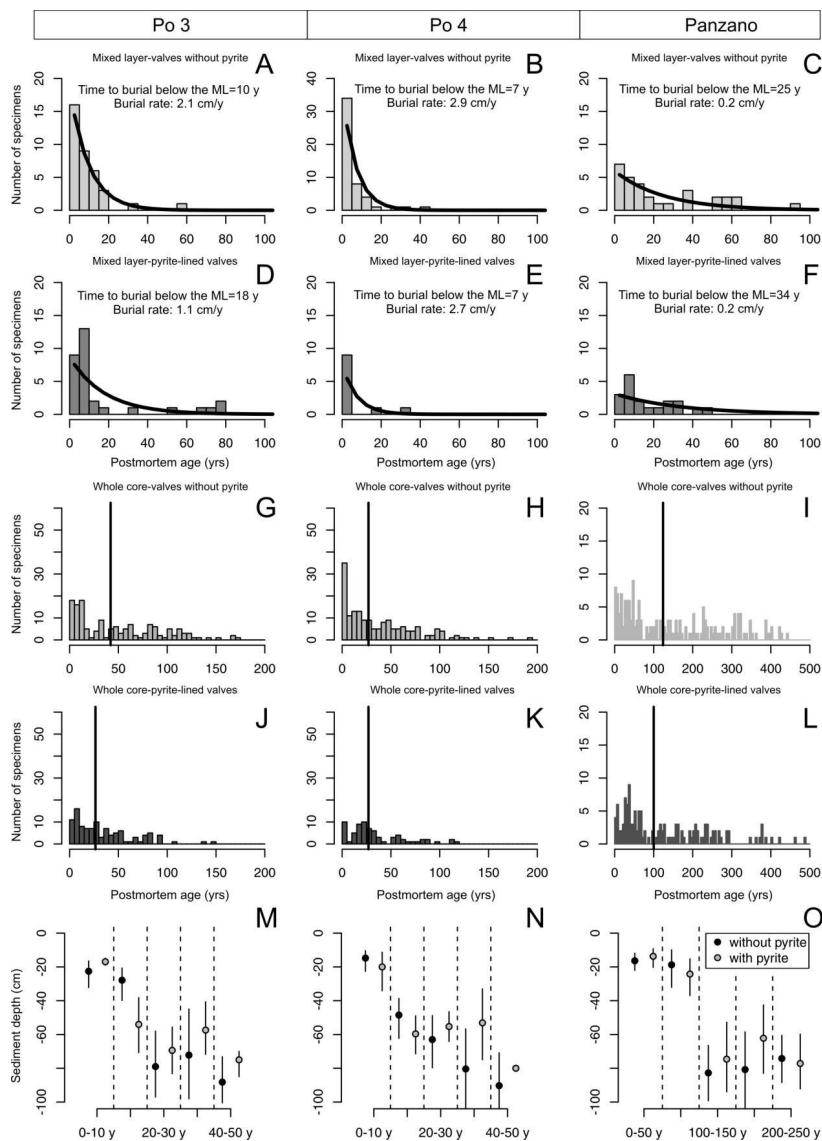
Figure 9 – A-L. Mixed-layer (A-F) and whole core distributions (G-L) of postmortem ages from Po 3, Po 4, and Panzano with valves with and without pyrite show that first, even the youngest valves less than 5-10 years old have pyritic linings. Second, the mixed-layer distributions of valves with and without pyrite show similar right-skewed shapes well-fitted by a simple disintegration-burial model (black lines) that indicate that both types of valves are burial below the mixed layer at a similar rate (time to loss corresponds to the mean age of the distribution). The time to valve loss is congruent with ^{210}Pb-based estimates of sediment accumulation, indicating that loss rates primarily correspond to burial rates. At the scale of whole cores, pyrite-lined valves exhibit a mode at ~25 years Po 4 and a mode at ~50 years at Panzano. M-O. Mean sediment depths of valves with (gray) and without pyrite (black) of the same age are similar. Both age and depth distributions indicate that the scenario that pyrite formation is not associated with deeper burial and occurs in reduced microniches in near-surface sediment zones.
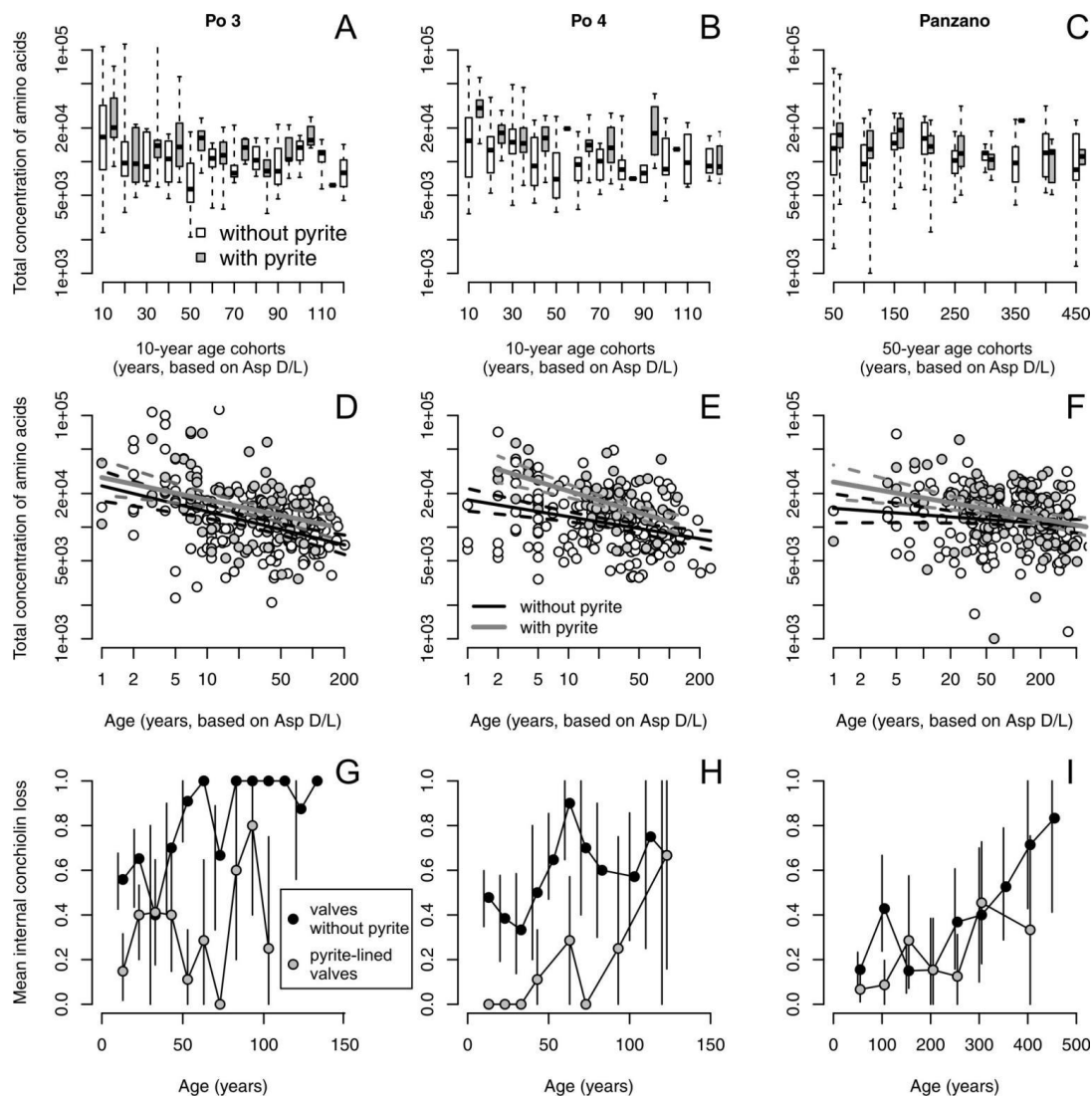
Figure 10 – A-C. Equally-old valves of *Varicorbula gibba* lined by pyrite tend to have higher concentrations of amino acids (visualized by boxplot pairs of valves with pyrite in gray boxes and without pyrite in white boxes) in the upper row, with age cohorts aggregated to 10 years at Po and 50 years at Panzano. D-F. Valves lined by pyrite possess higher intercepts of the linear dependence of log-transformed amino acid concentrations on log-transformed postmortem age than valves without pyrite. G-I. Valves lined by pyrite show higher mean frequency in preservation of periostracum or conchiolin layer than valves not lined by pyrite, with age cohorts aggregated to 10 years at Po and 50 years at Panzano.
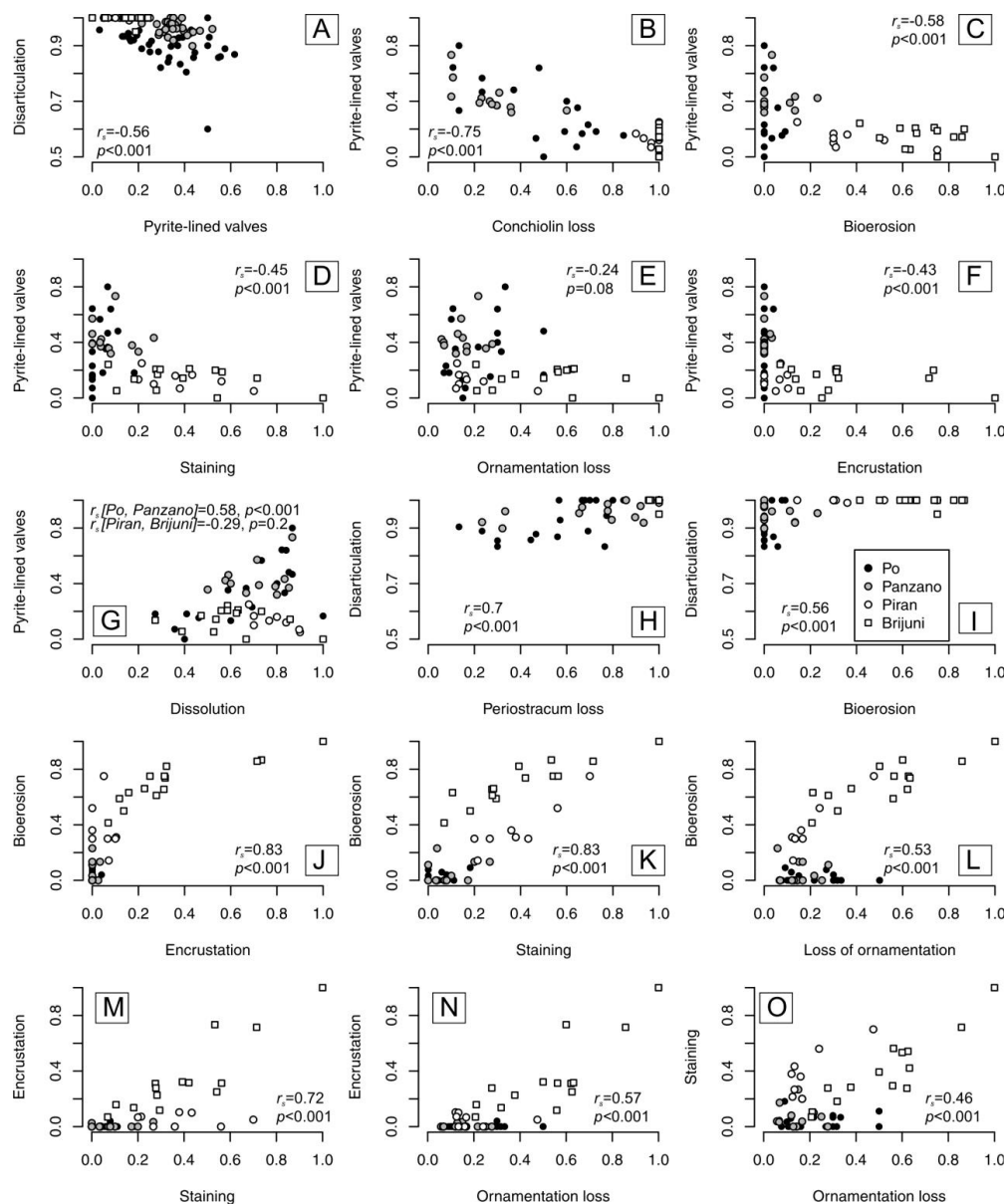
Figure 11. A-F. Negative relationships between per-increment frequencies of pyrite-lined valves and frequencies of other types of alteration (r_s values refer to Spearman rank correlations). G. The relation between frequencies of pyrite-lined valves and fine-scale dissolution depends on the site location and the pathway that ultimately leads to dissolution (pyrite oxidation at Po and Panzano or bioerosion at other site). Valves with pyrite commonly show internal fine-scale dissolution but are still associated with some surviving portions of periostracum or conchiolin layer. However, high frequencies of dissolved specimens are associated with low pyrite preservation as specimens from Piran and Brijuni are bored and dissolved but rarely associated with pyrite grains. H-L. Pairwise positive relationships between frequencies of disarticulation, conchiolin loss, bioerosion, encrustation, staining, and loss of ornamentation. M-O. Pairwise positive relationships between frequencies of encrustation, staining, and ornamentation loss.
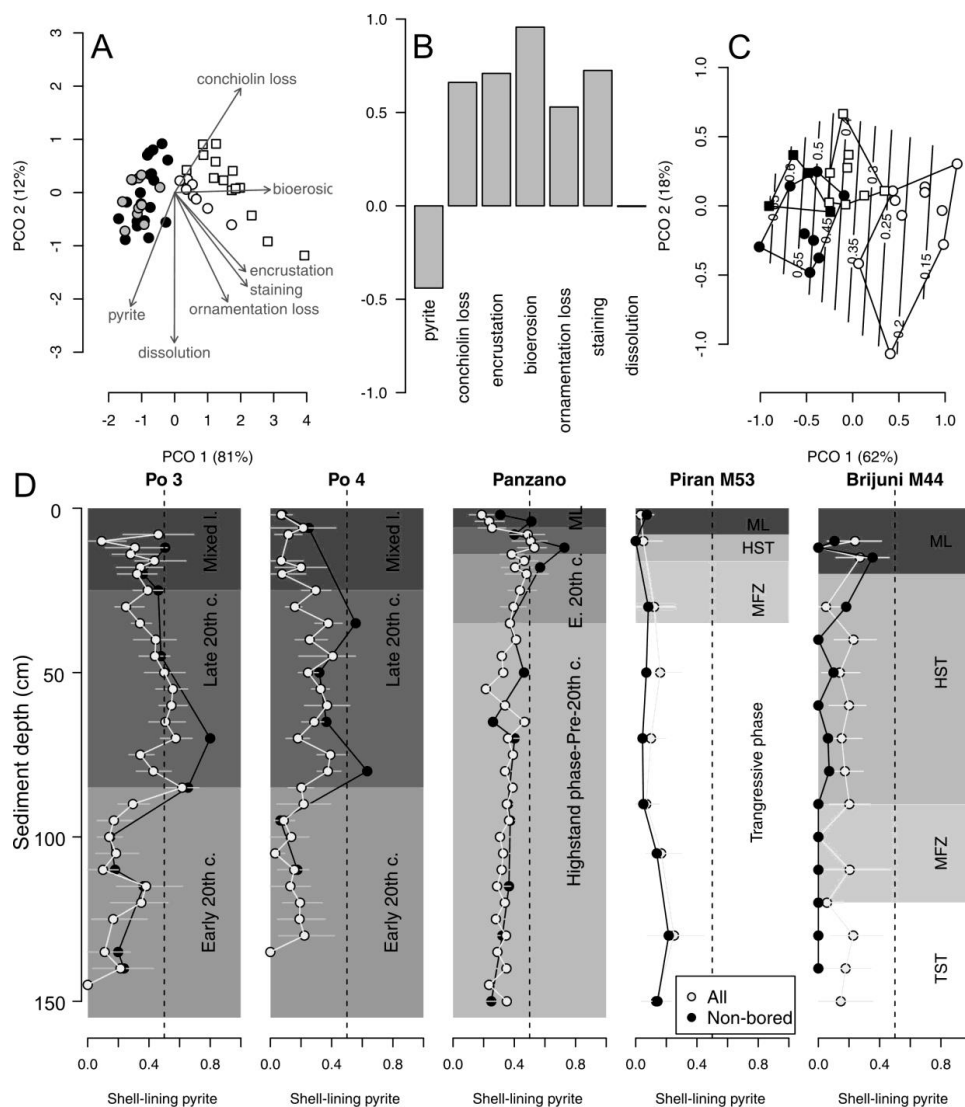
Figure 12 – A. Principal coordinate analysis (PCO) based on *V. gibba* alteration (using seven variables) in increments from all sites (excluding increments from the mixed layer). B. Correlations between PCO axis 1 and eight alteration variables show that pyrite varies inversely with other alteration variables. C. Principal coordinate analysis of increments Po and Panzano, showing the separation between the latest HST (white circles) and the late 20th century increments (black circles), mainly determined by the frequencies of pyrite-lined specimens (contours). D. Stratigraphic changes in the frequencies of all pyrite-lined valves (gray circles) of *V. gibba* peak at 40-50% in the upper part of cores at Po 3 and Po 4 and at 50% at ~10-20 cm at Panzano. The frequencies of pyrite-lined valves are typically less than 20% at Piran and Brijuni where sedimentation rates are slow. The frequencies of pyrite-lined valves at Piran and Brijuni further decline when the frequencies of pyrite-lined valves are limited to valves not affected by bioerosion (black circles), magnifying the contrast between well-preserved pyrite-lined valves at sites with high sedimentation (primary linings) and variably-preserved pyrite-lined valves at sites with slow sedimentation (with some pyrite corresponding to secondary linings).
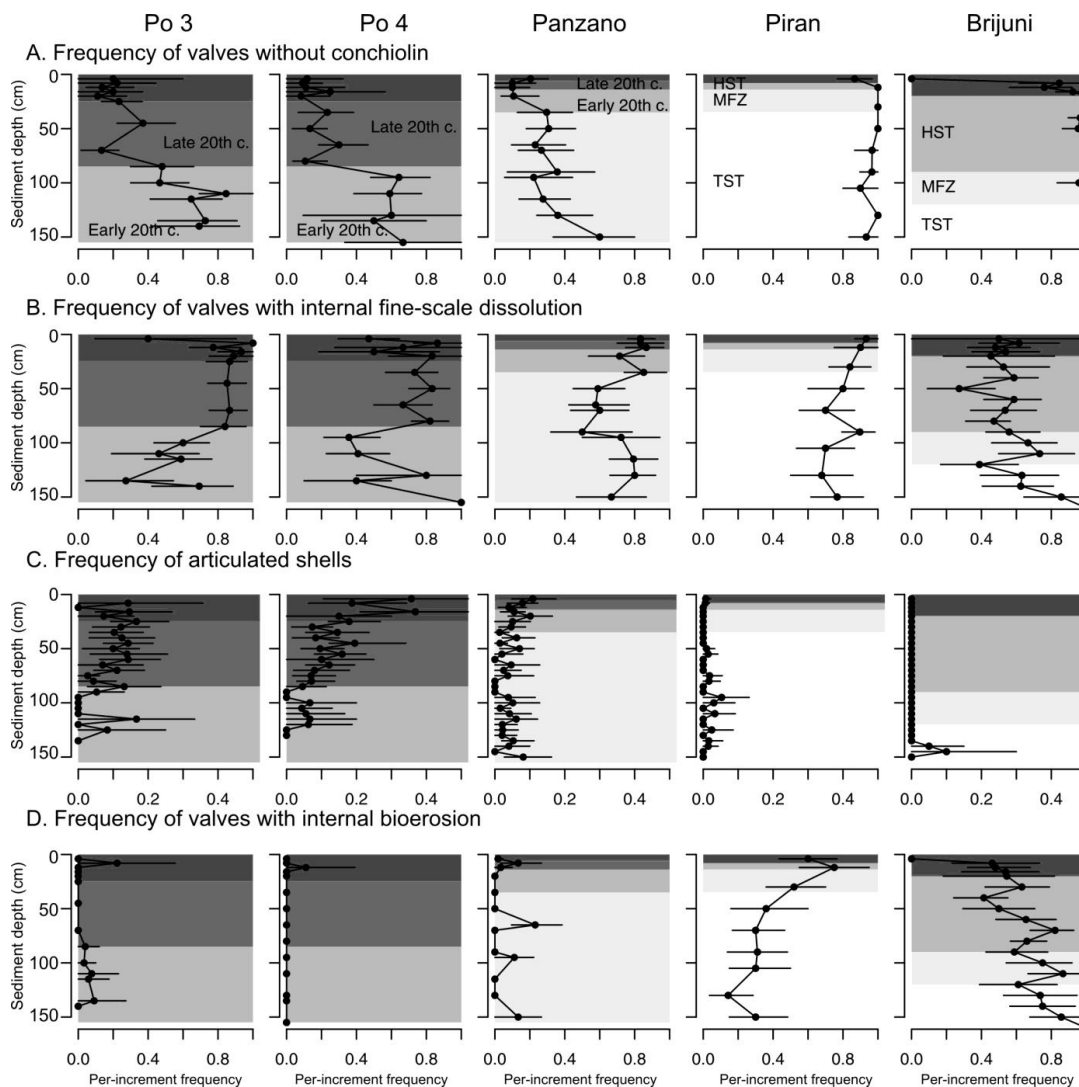
Figure 13 – Stratigraphic changes in the per-increment frequency of valves of *Varicorbula gibba* affected by the loss of conchiolin (A, external periostracum and internal conchiolin), by internal surficial fine-scale dissolution (B), characterized by the presence of articulation (C), and by internal bioerosion (D). TST – transgressive systems tract, MFZ – maximum flooding zone, HST – highstand systems tract.

1195
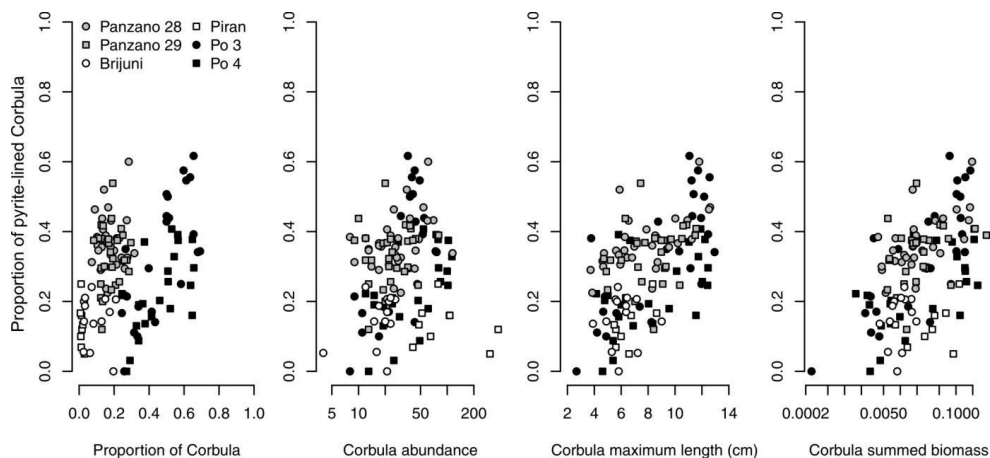
Figure 14 – The positive relationship between *V. gibba* biomass per increment and the frequency of valves lined by pyrite grains, interpreted to reflect the response of ecological and taphonomic processes as responding together to higher hypoxia frequency and a narrower extent of aerobic respiration in sediment, possibly linked by higher input of organics at times of

1200   mass mortalities and reduced mixing during the recovery. Within-core relationships show stronger relationships than regional-scale relationships that are affected by between-core differences in time averaging and thus absolute and proportional abundances are noisy.
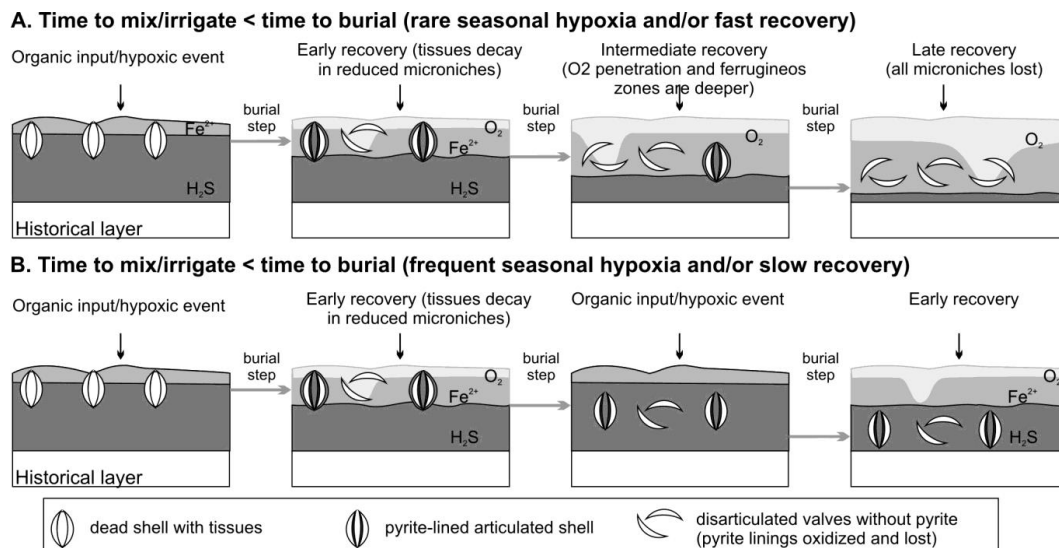
Figure 15 – Two pathways characterized by differences in the frequency of sediment organic enrichment and hypoxic events and/or by differences in recovery rate of infaunal communities with high mixing and irrigation potential. Both pathways promote the initial formation of reduced microniches when shallow-infaunal shells decay in sediments with iron-dominated pore water. A. In the aftermath of hypoxia, reduced microniches are formed initially, but these are recycled under recovery of infaunal communities that oxidize sediment and contribute to skeletal disintegration of initially articulated shells. B. If the frequency of hypoxic events associated with higher oxygen consumption is high, the oxic-anoxic interface repeatedly shallow within the sediment. The recovery of burrowing infauna is slow and bioirrigation remains patchy, and some subset of reduced microniches is thus not oxidized. Therefore, shells with pyrite linings can escape the mixed layer in the subsurface stratigraphic record even when the sediment fabric is bioturbated. In the historical layer, valves permanently remain in reducing conditions.

Table A1 – The results of fitting age-frequency distributions (with valves with and without pyrite) from the mixed layer at three stations to a simple disintegration model (with temporally-constant loss rate from the mixed layer) and to a
1220   sequestration model with three parameters. AICc - Akaike Information criterion corrected for sample size.

	Simple disintegration model (1 parameter)			Sequestration model (3 parameters)				
	Sample size (n)	lambda (loss from mixed layer)	Neg. log-likelihood	AICc	lambda1 (early loss from mixed layer)	lambda2 (late loss from mixed layer)	tau (sequestration)	Neg. log-likelihood	AICc
Po 3-without pyrite	36	0.1026	118.0	117.7	0.1176	0.0457	0.0037	238.1	242.2
Po 3-with pyrite	31	0.0558	120.5	116.8	0.1324	0.0233	0.0078	243.1	240.4
Po 4-without pyrite	50	0.1441	146.9	146.5	0.1674	0.0680	0.0061	295.8	299.5
Po 4-with pyrite	11	0.1358	33.0	32.5	0.2222	0.0723	0.0206	68.4	74.4
Panzano-without pyrite	30	0.0396	126.9	126.9	0.0421	0.0393	0.0963	255.9	260.7
Panzano-with pyrite	21	0.0296	94.9	91.7	0.0588	0.0080	0.0013	192.0	190.8